DOKUZ EYLUL UNIVERSITY
GRADUATE SCHOOL OF NATURAL AND APPLIED SCIENCES

PHOTOCHARACTERIZATION OF SOME CHROMOIONOPHORE STRUCTURES WITH FIBER OPTICS FOR SENSING PURPOSES

by
Mustafa TÜRE

August, 2008
İZMİR

PHOTOCHARACTERIZATION OF SOME CHROMOIONOPHORE STRUCTURES WITH FIBER OPTICS FOR SENSING PURPOSES

A Thesis Submitted to the
Graduate School of Natural and Applied Sciences of Dokuz Eylul University
In Partial Fulfillment of the Requirements for the Degree of Master of Chemistry

by
Mustafa TÜRE

August, 2008
İZMİR

M.Sc THESIS EXAMINATION RESULT FORM

We have read the thesis entitled **"PHOTOCHARACTERIZATION OF SOME CHROMOIONOPHORE STRUCTURES WITH FIBER OPTICS FOR SENSING PURPOSES"** completed by **MUSTAFA TÜRE** under supervision of **Assoc. Prof. KADRİYE ERTEKİN** and we certify that in our opinion it is fully adequate, in scope and in quality, as a thesis for the degree of Master in Chemistry.

Doç. Dr. Kadriye Ertekin

Supervisor

Doç. Dr. Kenan Dost	Prof.Dr. Kadir Yurdakoç
Jury Member	Jury Member

Prof.Dr. Cahit HELVACI

Director

Graduate School of Natural and Applied Sciences

ACKNOWLEDGMENTS

I would like to send my genuine thanks to my supervisor Associated Professor Dr. Kadriye Ertekin for providing the unique subject for my thesis, for her precious support during writing this thesis and for the great working conditions formed at our laboratory.

I gratefully acknowledge the invaluable help of my colleagues Özlem Öter and Sibel Derinkuyu.

I want to thank my parents and my wife without whose tolerant attitude to my working effort during the development of this dissertation I would go nowhere, and I also thank for their ceaseless support during all the years of my studies.

Mustafa TÜRE

PHOTOCHARACTERIZATION OF SOME CHROMOIONOPHORE STRUCTURES WITH FIBER OPTICS FOR SENSING PURPOSES

ABSTRACT

In the first part of this work, original Hg(II) sensor was tried to be developed by making use of 4-{ (1E, 3E)-3-[(4- chloro-phenyl)imino]-1-propenyl}-N,N-dimetilanilin (CPIPA), a newly synthesized indicator dye. CPIPA, was spectrophotometrically characterized in various solvents and ionic liquids. Spectral response of dye to dissolved mercury and pH and was considered. The complex stoichiometry between dye and heavy metal was defined. In addition to that, the transformation of spectral response by time was studied.

In the second part, an original Al^{3+} probe was tried to be developed. Organic fluoroionophore; N-N'-bis (2-hydroxybenzylidene)-ethane-1,2-diamine (Y1), was studied in various solvents (dichlorometan, tetrahydrofurane, toluen and ethanol) by using absorption and emission spectroscopy.

In all sensor designs, sensor response, stoichiometry of possible complex between the fluoroionophore and metal cation, possibility of regeneration, detection limit, linear working range and repeatability were defined by using absorption and emission based spectrophotometric techniques.

Key Words: optic sensors, photo-characterization, polyvinyl chloride, organic fluoroionophore, Hg (II) and Al (III).

BAZI KROMOİYONOFOR YAPILARININ SENSÖR GELİŞTİRME AMAÇLI OLARAK OPTİK FİBERLER İLE FOTOKAREKTERİZASYONU

ÖZ

Bu çalışmanın birinci bölümünde, yeni sentezlenen bir indikator olan 4-{(1E, 3E)-3-[(4-klorofenil)imino]-1-propenil}-N,N-dimetilanilin (CPIPA) kullanılarak orijinal Hg(II) sensörü geliştirilmeye çalışıldı. CPIPA çeşitli çözelti ortamlarında ve iyonik sıvıların içerisinde spektrofotometrik olarak karakterize edildi. Boyanın pH'a ve çözünmüş civaya olan spektral yanıtları değerlendirildi. Boya ile ağır metal arasındaki oluşması muhtemel kompleksin stokiyometrisi belirlendi. .Ayrıca spektral yanıtın zamana bağımlı olarak değişimi incelendi.

İkinci bölümde ise, orijinal Al^{3+} sensörü geliştirilmeye çalışıldı. Al^{3+}'e seçimli organik floroiyonofor, N-N'-bis (2-hydroxybenzylidene)-ethane-1,2-diamine (Y1), farklı çözücülerde (diklorometan, tetrahidrofuran, toluen ve etanol) ve çeşitli tampon çözelti ortamlarında, absorpsiyon ve emisyon spektroskopisi kullanılarak araştırıldı.

Tüm sensör tasarımlarında, sensör yanıtı, floroiyonoforun metal katyonuyla oluşturabileceği muhtemel kompleksin stokiyometrisi, rejenere edilebilirliği, tayin limiti, doğrusal çalışma aralığı ve tekrarlanabilirlik özellikleri belirlendi.

Anahtar Kelimeler: optik sensörler, fotokarekterizasyon, polivinil klorür, organik floroiyonofor, Hg (II) ve Al (III).

CONTENTS

Page

CHAPTER ONE

INTRODUCTION

1.1 Chemical Sensors

"A chemical sensor is a device that transforms chemical information ranging from the concentration of a specific sample component to total composition analysis into analytical useful signal. The chemical information mentioned above may originate from a chemical reaction of the analyte or from a physical property of the system investigated. A chemical sensor is an essential component of an analyzer. In addition to the sensor, the analyzer may contain that perform the following functions: sampling, sample transport, signal processing, data processing" (Wolfbeis, 1991).

Chemical sensors have been widely used in such applications as critical care, safety, industrial hygiene, process controls, product quality controls, human comfort controls, emissions monitoring, automotive, clinical diagnostics, home safety alarms, and, more recently, homeland security. In these applications, chemical sensors have resulted in both economic and social benefits. Chemical sensors have a chemical or molecular target to be measured. Sensors can be classified in many different ways. They may be classified according to the principle of operation of the transducer in two main groups as "physical" and "chemical" sensors. They also can be divided into sub groups as optical, electrochemical, electrical, mass sensitive, magnetic and thermometric devices. They can also be classified as direct and indirect sensors or as reversible or non-reversible ones and in respect of their applications or sizes (Oter, 2007).

1.1.1 Classification of Chemical Sensors (Hunicki et al.,1991)

Chemical sensors may be classified according to the operating principle of the transducer.

1. Optical devices transform changes of optical phenomena, which are the result of an interaction of the analyte with the receptor part. This group may be further subdivided according to the type of optical properties which have been applied in chemical sensors:

a) absorbance, measured in a transparent medium, caused by the absorptivity of the analyte itself or by a reaction with some suitable indicator.

b) reflectance is measured in non-transparent media, usually using an immobilized indicator.

c) luminescence, based on the measurement of the intensity of light emitted by a chemical reaction in the receptor system.

d) fluorescence, measured as the positive emission effect caused by irradiation. Also, selective quenching of fluorescence may be the basis of such devices.

e) refractive index, measured as the result of a change in solution composition. This may include also a surface plasmon resonance effect.

f) optothermal effect, based on a measurement of the thermal effect caused by light absorption.

g) light scattering, based on effects caused by particles of definite size present in the sample.

The application of many of these phenomena in sensors became possible because of the use of optical fibers in various configurations. Such devices have also been called optodes. It should be emphasized that fiber optics now commonly used are only technical devices applicable in a large group of optical sensors which can be based on various principles.

2. Electrochemical devices transform the effect of the electrochemical interaction analyte – electrode into a useful signal. Such effects may be stimulated electrically or may result in a spontaneous interaction at the zero-current condition. The following subgroups may be distinguished:

a) voltammetric sensors, including amperometric devices, in which current is measured in the d.c. or a.c. mode. This subgroup may include sensors based on chemically inert electrodes, chemically active electrodes and modified electrodes. In this group are included sensors with and without (galvanic sensors) external current source.

b) potentiometric sensors, in which the potential of the indicator electrode (ion-selective electrode, redox electrode) is measured against a reference electrode.

c) chemically sensitized field effect transistor (CHEMFET) in which the effect of the interaction between the analyte and the active coating is transformed into a change of the source-drain current. The interactions between the analyte and the coating are, from the chemical point of view, similar to those found in potentiometric ion-selective sensors.

d) potentiometric solid electrolyte gas sensors, differing from class 2b) because they work in high temperature solid electrolytes and are usually applied for gas sensing measurements.

3. Electrical devices based on measurements, where no electrochemical processes take place, but the signal arises from the change of electrical properties caused by the interaction of the analyte.

a) metal oxide semiconductor sensors used principally as gas phase detectors, based on reversible redox processes of analyte gas components.

b) organic semiconductor sensors, based on the formation of charge transfer complexes, which modify the charge carrier density.

c) electrolytic conductivity sensors.

d) electric permittivity sensors.

4. Mass sensitive devices transform the mass change at a specially modified surface into a change of a property of the support material. The mass change is caused by accumulation of the analyte.

a) piezoelectric devices used mainly in gaseous phase, but also in solutions, are based on the measurement the frequency change of the quartz oscillator plate caused by adsorption of a mass of the analyte at the oscillator.

b) surface acoustic wave devices depend on the modification of the propagation velocity of a generated acoustical wave affected by the deposition of a definite mass of the analyte.

5. Magnetic devices based on the change of paramagnetic properties of a gas being analyzed. These are represented by certain types of oxygen monitors.

6. Thermometric devices based on the measurement of the heat effects of a specific chemical reaction or adsorption which involve the analyte. In this group the heat effects may be measured in various ways, for example in the so called catalytic sensors the heat of a combustion reaction or an enzymatic reaction is measured by use of a thermistor. The devices based on measuring optothermal effects (If) can alternatively be included in this group.

7. Other physical properties as for example X-, p- or r- radiation may form the basis for a chemical sensor in case they are used for determination of chemical composition. This classification represents one of the possible alternatives. Sensors have, for example, been classified not according to the primary effect but to the method used for measuring the effect. As an example can be given the so-called catalytic devices in which the heat effect evolved in the primary process is measured by the change in the conductivity of a thermistor. Also, the electrical devices are often put into one category together with the electrochemical devices.

Sensors have also been classified according to the application to detect or determine a given analyte.

Examples are sensors for pH, for metal ions or for determining oxygen or other gases.

Another basis for the classification of chemical sensors may be according to the mode of application, for example sensors intended for use in vivo, or sensors for process monitoring and so on.

1.1.2 Advantages and Disadvantages of Chemical Optical Sensors (Wolfbeis, 1991).

There are numerous advantages of chemical optical sensors described below.

- Optical sensors do not require a reference signal as in potentiometry which increases the cost and causes perturbations.
- The ease of miniaturization allows the development of very small, light and flexible sensors much smaller than any electrochemical sensor especially for sensing in clinical chemistry and medicine.
- Low loss optical fibers allow transmittance of optical signals over wide distances. Remote sensing makes it possible to perform analyses when samples are hard to reach, dangerous, too hot or too cold, in harsh environments or radioactive.
- They are not influenced from electrical interferences, strong magnetic fields and surface potentials. On the other hand fibers do not present a risk for health since they do not disperse any electrical signal.
- Analyses can be performed in almost real time without any need of sampling.
- Since several fiber sensors placed in different sites can be coupled to one fluorometer, the method allows multiple analyses with a single control instrument.
- Coupling of small sensors for different analyte to produce a sensor bundle of small size allows simultaneous monitoring of various analyte without any interference.
- Extremely small sample volume is not a disadvantage as in polarographic electrodes.
- Fiber optical sensing is a non-destructive analytical method.
- Fibers are manufactured from non-rusting materials, so that they have excellent stability. They are also resistant to radiation.

- In practice, a single fiber may be used to assay several analyte at the same time.
- Especially sensors based on dynamic fluorescence quenching have a useful dynamic range often larger than that of electrochemical sensors.
- Most fiber sensors can be employed over a wider temperature range than electrodes.

Besides these advantages optical sensors also have some disadvantages:

- Ambient light can interfere so optical isolation is necessary.
- They have limited long term stability because of photobleaching and wash out. The signal drifts due to these reasons can be compensated by using ratiometric method or time resolved measurements.
- The fiber optics used at present have impurities that can give background absorption, fluorescence and Raman Scatter. Low-priced (plastic) fibers are confined to visible range, whereas UV light is transmitted by rather expensive quartz fibers only. Because of this sensing dyes that can be excited at visible range are preferred in sensor designs.
- More selective indicators have to be found for various important analyte and the immobilization techniques have to be improved.

In summary, optical sensors offer a variety of new aspects. Despite several limitations, they have the potential of becoming an attractive alternative to other sensing methods and to perform diagnostic, environmental or clinical functions better, faster, more accurate or less expensive than existing approaches.

1.1.3 Fiber Optical Chemical Sensors and Optodes

They have become an important area of research since their introduction two decades ago. Optical sensors are compact and ideally suited to miniaturization while at the same time they are resisting to electrical interference and utilize the simplicity of photometric measurements. Many optical chemical sensors utilize color complexing or redox reagents immobilized in suitable polymeric membrane (Ensafi

& Bakhshi, 2003; Ensafi & Aboutalebi, 2005). Optical chemical sensors can be classified in three groups: Probes, fiber-optic chemical sensors and non fiber optic chemical sensors. Sensors which produce an irreversible response to the presence of analytes are referred to as 'probes'. If the signal is reversible and continuous then it is called as sensor. Fiber optic sensors are based on optical spectroscopy performed on sites inaccessible to conventional spectroscopy, over large distances, or even on several spots along the fiber (Oter, 2007). Schematic structure of an optical fiber and light propagation is shown in Figure 1.1.

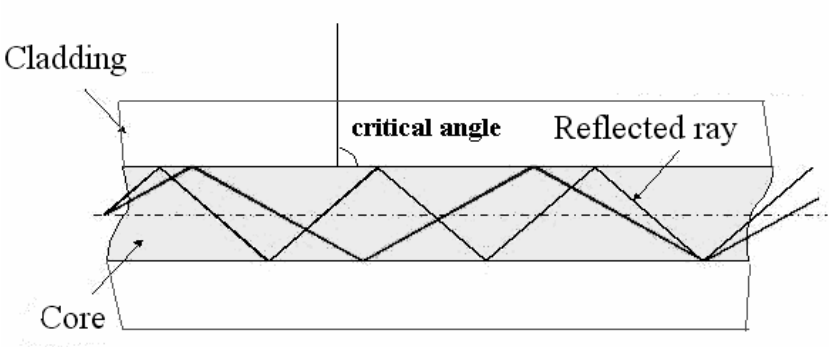

Figure 1.1 Structure of an optical fiber.

1.1.3.1Direct Fiber Optic Sensors

In these sensors, the intrinsic absorption of the analyte is measured directly. No indicator chemistry is involved. Thus, it is more a kind of remote spectroscopy, except that "the instrument comes to the sample" (rather than the sample to the instrument or cuvette). Numerous geometries have been designed for plain fiber chemical sensors, all kinds of spectroscopies (from IR to mid-IR and visible to the UV; from Raman to light scatter, and from fluorescence and phosphorescence intensity to the respective decay times) have been exploited, and more sophisticated methods including evanescent wave spectroscopy and surface plasmon resonance have been applied (Wolfbeis, 2006).

In the late 1980s, as sensing method known as distributed sensing became known. This enabled chemical analyses to be performed along the distance of an optical fiber

and has meanwhile been applied to monitor the quality of river water along a fiber cable and to detect gas and oil leakage along oil and gas pipelines, to mention only two examples(Wolfbeis, 2006).

1.1.3.1.1 Direct Sensors Based on Absorption or Fluorescence. Fiber optics have been used mainly to remotely sense chemical species via their intrinsic absorption or fluorescence. Methane and other hydrocarbons were a target analyte from the beginning. They can be detected by infrared spectroscopy in the gas phase. The detection limit was 2000 ppm, which is 4 % of the lower explosion limit of methane, there by demonstrating that fully remote sensing is possible and can be used for the surveillance of flammable and explosive gases in industrial and mining complexes as well as in residential areas (Wolfbeis, 2006).

In subsequent work, differential absorption spectroscopy was applied. This 2 wavelength approach enables direct detection of differential absorption signals of specific overtone bands of methane. Later on, a 10-km long fiber cable was described that permits remote sensing of methane gas by near infrared absorption. An ultralow-loss silica optical fiber and a compact absorption cell in conjunction with highly radiant light emitting diodes in the near IR region. The bands at around 1.33 and 1.66 μm were analyzed (Wolfbeis, 2006).

Finally, an all-optical remote gas sensor system was reported for methane and propane that works over a 20-km range. In context with methane detection during offshore oil drilling, another infrared fiber optic methane sensor was reported. The detector comprises 3 main units: a microcomputer-based signal processing and control unit, a nonconducting fiber optic gas sensor, and an optical fiber cable module. The system operates at an absorption line of methane where silica fibers have very low losses. Unlike methane and the other alkanes, aromatic hydrocarbons have absorptions in the UV part of the spectrum, and thus may be detected through UV spectrometry using silica fibers. This scheme is useful for "aromatic" water pollutants such as toluenes and xylenes with their absorption bands between 250 and

300 nm. Similarly, nitrate anion can be monitored (albeit with low sensitivity) in water via its UV absorption at 250 nm (Wolfbeis, 2006).

In principle, any chemical species that absorbs UV-Vis light can be "sensed" by fiber optic (“remote”) absorption spectrometry which is interfered by any other species that absorbs at the same wavelength. A fiber optic absorption cell was described for remote determination of the blue copper ion in industrial electroplating baths. The sensor consists of an absorption cell which resides in the plating bath, and utilizes fiber optics to direct light into and out of the cell. The sensor can be placed in strong sulfuric acid for weeks to years. The light source and detection electronics can be maintained in a controlled environment and can be multiplexed to several sensors of similar design, if desired (Wolfbeis, 2006) .

The sensor operates by measuring the blue-green absorbance of Cu^{2+} ion with a near-IR light emitting diode (820 nm) as the light source. The device is capable of measuring copper(II) ion concentrations from 50 mM to 500 mM with relative standard deviations of less than 1%.The feasibility of an optical fiber system was demonstrated for the differential absorption analysis of the car pollutant nitrogen dioxide. It absorbs in the visible and can be "sensed" using an Ar-ion laser. The yellow metabolite bilirubin has been monitored in blood via fiber optic spectrometry in serum. The tip of a fiber optic cable was inserted into a injection needle so to reach the blood sample, and absorbance (and later fluorescence) was acquired of a sample contained in the cavity at the tip of the fiber or needle (Wolfbeis, 2006).

Another milestone paper was the one by Newby et al. on remote spectroscopic sensing of chemical adsorption via evanescent wave spectroscopy using a single multimode optical fiber. Declad single fibers were developed for collecting evanescently excited fluorescent signals from solutions. It was shown that the sensor is particularly useful for studying species adsorbed onto the sensor surface, for example dye-labeled proteins. Also, Raman data from benzene were collected to indicate its sensitivity in the bulk mode. (Wolfbeis, 2006)

1.1.3.1.2 Early Refractometric Sensors. Refractometry is as unspecific as is absorption spectrometry, but has its merits if applied under well-characterized conditions. In 1984, Haubenreisser et al. reported on (a) the relation between transmission and refractive index characteristics, (b) the sensitivity, and (c) the working range of a fiber optic refractometer of mixtures of fluids. The U-shaped fiber refractometer was shown to be useful for various physical quantities that vary with refractive index (Wolfbeis, 2006).

Another early fiber optic refractive "sensor" was the one for measurement of temperature and salinity variations of sea water. The sensing region consisted of a partly uncovered light guide. It detects salinity variations in water of known temperature, and temperature variations in water of known salinity with an accuracy of +/- 2 g/L and 1 °C**,** respectively, at NaCl concentrations of 300 g/L. Resonant photoacoustic gas spectrometry was adapted to fiber optic sensor technology as early as in 1984. A Mach-Zehnder arrangement was combined with a resonant photoacoustic cell for gap analysis. The pollutant gas NO_2 was detectable in a concentration of 0.5 ppm. In a smart optical fiber hydrogen sensor, the fiber is coated with palladium metal which expands on exposure to hydrogen. This changes the effective optical path length of the fiber, which is detected by interferometry (Wolfbeis, 2006).

1.1.3.2 Indirect Fiber Optic Chemical Sensors

“This section covers early indirect fiber optic chemical sensors (FOCS) for species that cannot be sensed directly but require the use of indicators, probes, labeled biomolecules, or color-forming reactions” (Wolfbeis, 2006).

1.1.3.2.1 Sensors for (dissolved) Gases. The use of simple optical technology to devise reflective sensor devices for the monitoring of dissolved and atmospheric gases and vapors are under investigation.

Current investigations include the detection of traces of toxic gases such as NH_3, H_2S, Cl_2, SO_2, HCHO, HCl, etc. and also other gases such as O_2 using chemically sensitive matrices that can be interfaced to the optical fibers to produce devices that will have probe configurations and employ reflectance or fluorescence detection techniques at the chemical transducer. Recent works include the investigation into organic and organometallic optical thin films for gas sensors. Thin film devices are produced by sputtering, vacuum sublimation and Langmuir-Blodgett techniques.

Multi-gas and vapor sensing systems are being studied which utilize differences in spectra and chemical kinetics, in conjunction with novel signal processing techniques. (Wolfbeis, 2006)

1.1.3.2.2 pH Sensors. As stated above, the beginning of optical pH sensor technology remains hidden. What is nowadays referred to as a sensor layer was formerly mostly referred to as a test strip, a dry reagent chemistry, or an immobilized reagent.

A general logic that is based on the immobilization chemistry of commercial reflectometric test strips was presented and extended to various pH ranges. Such sensing "chemistries" are easily produced and can been coupled to fiber optics. This enabled sensing to be performed at formerly inaccessible sites. Peterson et al. were the first to report on a fiber optic pH sensor. The system comprised plastic fibers, a pH chemistry at their end (composed of a cellulosic dialysis tubing filled with a mixture of polystyrene particles and polyacrylamide beads dyed with phenol red), LED light sources, and photodiodes. The system is operated at two wavelengths. *Fig. 1.2* gives a schematic of the fiber tip (Wolfbeis, 2006).

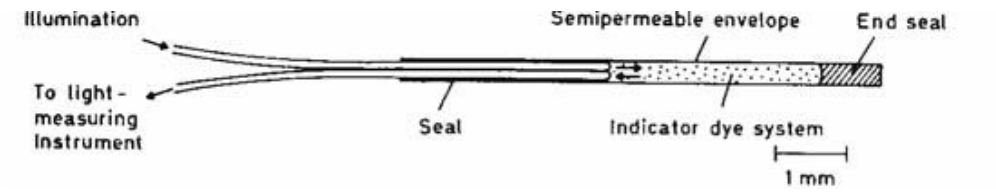

Figure 1.2 First fiber optic pH sensor for in vivo use.

As the potential of optical fiber probes for pH measurements was rapidly recognized, several other articles appeared within a few years. Most were reflectance-based, and Seitz reported the first fluorescent pH sensors. The article by Janata on whether pH optical sensors can really measure pH is another "must" in the early literature since it points to aspects hardly addressed in pH sensor work (Wolfbeis, 2006).

The dependence on ionic strength is an intrinsic limitation of pH sensors using indicator dyes. Opitz and Lübbers and Offenbacher et al. have presented solutions to this by making use of two indicators whose dependency of their pKa on ionic strength is different, so that two independent signals are obtained from two dyes or sensors. Given the advantages of diode lasers operated at wavelengths of above 600 nm, respective pH probes were used. Abraham et al. applied the probe of Peterson et al. successfully to monitoring intra-arterial pH in dogs even under extremes of physiological conditions. The difference between fiber optic and electrode pH gave a maximal difference of 0.12 pH units. (Wolfbeis, 2006)

1.1.3.2.3 Sensors for Anions. Nitrate has an intrinsic absorption at around 250 nm that may be used for sensing it in drinking water. However, practically all other matrices have such a strong background absorption in the UV that sensing of nitrate (and of any other UV absorbing species) is impossible. Other schemes are therefore needed. Anions such as chloride, nitrate, but also salicylate and penicillinate can be detected by the co-extraction method ("anion in – proton in") using phase transfer agents such as tetralkylammonium salts (Wolfbeis, 2006).

In contrast to extraction processes on electrodes, those occurring in optical sensor membranes require complete mass transfer. The scheme can be made pH independent. The fact that halides and pseudohalides quench the fluorescence of certain dyes as reported by Stokes in 1869 was used to optically sense halides. It displays selectivity due to the use of an enantioselective carrier (Wolfbeis, 2006).

The ion sensing scheme based on the use of potential-sensitive or polarity-sensitive dyes (PSDs) was extended to other anions. Both the clinically significant chloride ion and the environmentally important nitrate anion can be sensed in the desired concentration ranges. Such sensors have the unique advantage of having a virtually pH-insensitive response. (Wolfbeis, 2006)

1.1.3.2.4 Sensors for Alkali and Earth Alkali Ions. It appears that Charlton et al. have discovered the first methods for reversible and continuous optical measurement of the clinically highly important alkali and earth alkali ions. In one approach they use plasticized poly (vinyl chloride) along with valinomycin as the ion carrier, and a detection scheme that was later referred to as co-extraction. In their system, potassium ion is extracted into plasticized PVC, and the same quantity of the anionic red dye erythrosine is co-extracted into it. The extracted erythrosine is quantified via absorbance or reflectance (Wolfbeis, 2006).

Charlton also discovered the ion exchange principle. Again they used a plasticized PVC film containing valinomycin and - in addition – a deprotonable dye (MEDPIN; a lipophilic 2,6-dichlorophenol-indophenol). On extraction of potassium from the sample into the sensor membrane a proton is released from MEDPIN which then turns blue. The sensor layer measures potassium over the clinical range with excellent performance. This scheme proved to be highly flexible. The dye used in the commercial system is superior (in terms of stability) to other dyes such as Nile Blue that later have been applied in the ion exchange detection scheme. (Wolfbeis, 2006)

While heavy metals can be easily detected by making use of known indicator dyes or quenchable probes, the alkali and earth alkaline elements are not easily recognized by conventional dyes at neutral pH and room temperature, and without addition of reagent. Therefore the molecular recognition properties of crown ethers and cyclic peptides have been widely used (Wolfbeis, 2006).

The first studies were made by co-extraction of ions from water into chlorinated hydrocarbons, but later on the reagents were dissolved in plasticized PVC. The

amberlite ion exchanger (of the XAD type) is another widely used matrix for immobilizing indicator probes. Crown ethers have excellent recognition properties and can recognize numerous ions including alkali ions. Unfortunately, those synthesizing new crown ethers tend to investigate their properties in organic solutions such as acetonitrile and then claim that the findings may be useful for sensing alkali ions, thus ignoring the fact that alkali ions usually are sensed in aqueous solutions (including blood) where binding constants are very different. An interesting scheme for an optical sensor for sodium and based on ion-pair extraction and fluorescence was introduced by the Seitz group (Wolfbeis, 2006).

The chromo- and fluoro-ionophores form a particularly interesting class of probes since they can combine recognition properties with optical transduction such as changes in color or fluorescence. Chromo-ionophores are being used in clinical test strips for K^+ since 1985 and based on the work of Voegtle and others. The fluorescence of many fluorophores is particularly sensitive to perturbations of its microenvironment. For example, the photo-induced electron transfer (PET) can be suppressed on binding alkali ions. This has been demonstrated in impressive work by the groups of Valeur and DeSilva. Most noteworthy, the fluoro-ionophores are contained in a hydrophilic rather than hydrophobic matrix. The fluoroionophores are used in Roche's and Osmetech's Opti-1 clinical electrolyte analyzer (Wolfbeis, 2006).

A novel approach for ion sensing is based on the use of potential sensitive or polarity-sensitive dyes (PSDs) and was presented first in 1987. PSDs are charge dyes and typically located at the interface between a lipophilic sensor phase and a hydrophilic sample phase. The transport of an ion into the lipophilic sensor layer causes the PSD to be displaced from the hydrophilic/hydrophobic interface into the interior of the respective phase (or vice versa), thereby undergoing a significant change in its fluorescence properties. (Wolfbeis, 2006)

1.1.3.2.5 Sensors for Heavy Metal Ions. It has been known for many years that metal ions can be detected qualitatively by immobilizing indicator dyes on solid supports such as cellulose.

In fact, this approach forms the basis for the widely used test strips for heavy metals. Again, Zhujun and Seitz appear to have been the first to exploit this scheme to FOCS. The sensor described responds to Al^{3+}, Mg^{2+}, Zn^{2+} and Cd^{2+} and was prepared by immobilizing quinolin-8-ol-5-sulfonate (QS) on an ion-exchange resin and attaching the resin to the end of a trifurcated fiber-optic bundle. The weak fluorescence of QS is strongly enhanced on complexation of metal ions. Detection limits for the metal ions are all <1x10-6 M. Immobilized and dissolved QS behave similarly with respect to pH and interferences. Other metal ion sensing schemes were reported by the same group (Wolfbeis, 2006).

Numerous other FOCS schemes have been described for heavy metals in the past 20 years (for reviews, see). In looking at the more recent literature one may state, however, that some of the newly described "chemistries" perform hardly better than the rather old commercial systems based on the use of dry reagent chemistries, with the additional advantage that they are compatible with a single instrument for read-out (Wolfbeis, 2006).

In fact, some of the newer systems involve rather extensive chemistry and – worst of all – seem to strongly differ in terms of spectroscopy and analytical wavelengths so that they all require their own opto-electronic platform. On the other hand, there is substantial need for (low-cost) sensors for less common species, and those for Al3+ and certain heavy metals are typical examples. (Wolfbeis, 2006)

1.1.4 Polymeric Supports and Coatings Used For Optic Sensor Designs

1.1.4.1 Lipophilic Polymers and Plasticizers

Polymers that have a high glass transition temperature (Tg) are brittle (Figure 1.3). They require plasticizers to make them flexible. Furthermore, the high density/rigidity of the polymer chains (without plasticizers) hinders diffusion of ions and gases in the polymer matrix. Therefore, plasticizer to polymer ratios of up to 2:1 is required. While polyvinylchloride (PVC) is soluble in tetrahydrofuran and cyclopentanone, polymers such as methacrylate, polystyrene and polyvinyl acetate are also soluble in ethyl acetate, ethylmethyl ketone, dichloromethane, etc.

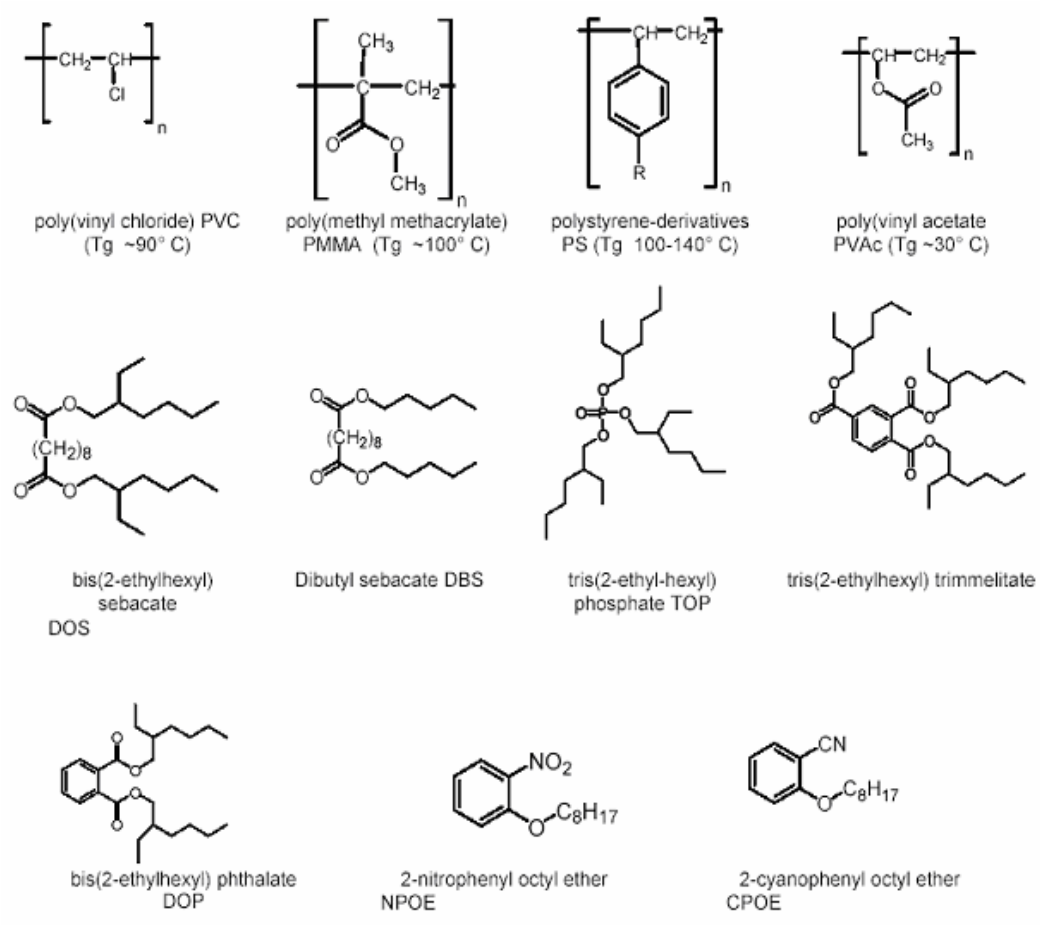

Figure 1.3 Lipophilic Polymers and Plasticizers that have a high glass transition temperature (taken from http://www2.uni-jena.de/~c1moge/Mohr/ASCOS2002. pdf).

Polymers with low glass transition do not require plasticizers (Figure 1.4). However, these compounds are often apolar and, consequently, bad solvents for polar ligands, ionophores, dyes, and analytes.

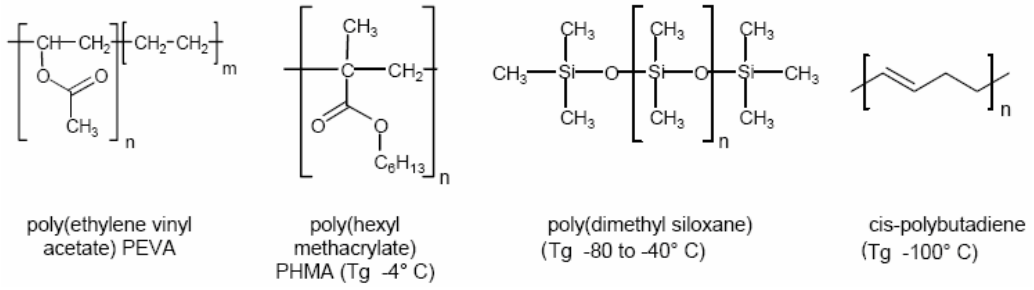

Figure 1.4 Polymers with low glass transition (taken from http://www2.uni-jena.de/~c1moge/Mohr/ASCOS2002.pdf).

Gankema, Lugtenberg, Engbersen, Reinhoudt & Moller (1994) have presented siloxane copolymers with reactive methacrylate groups and polar substituents which exhibit a behaviour and polarity similar to plasticized PVC but have the advantage that all components can be covalently linked to the polymer matrix (by copolymerisation) (Oter, 2007).

1.1.4.2 Hydrophilic Polymers

Hydrophilic polymers provide a matrix which corresponds to an aqueous environment (Figure 1.5). Ions can diffuse quite freely, but the possible water uptake (10-1000%) can cause significant swelling of the polymer. Swelling of the matrix affects the optical properties of the sensors and, consequently, the signal changes.

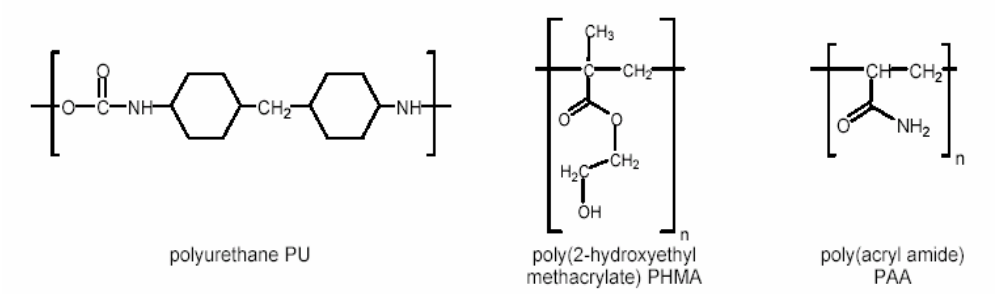

Figure 1.5 Hydrophilic polymers (taken from http://www2.uni-jena.de/~c1moge/Mohr/ASCOS2002.pdf).

1.1.4.3 Ionic Polymers (polyelectrolytes)

Polyelectrolytes exhibit a large amount of dissociable groups. These compounds are often used for ion exchange chromatography. They can also be used to exchange their counterions with indicator ions (Figure 1.6).

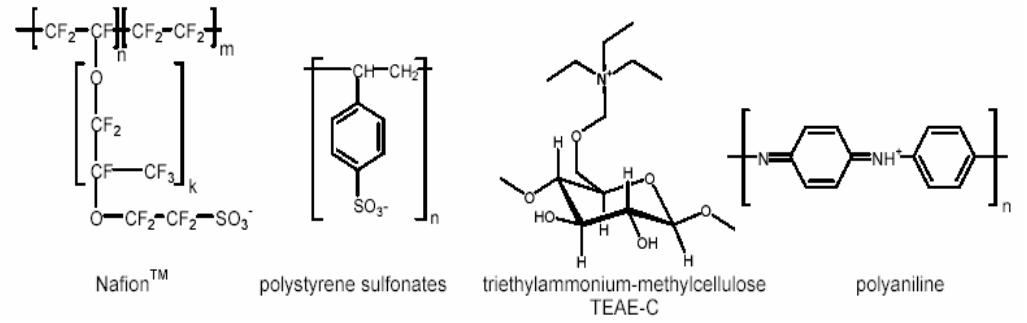

Figure 1.6 Ionic Polymers.(taken from http://www2.uni-jena.de/~c1moge/Mohr/ ASCOS2002.pdf)

1.2 Ionic Liquids (Yang & Pan, 2005)

Ionic liquids are very new matrix materials for sensor design. Unlike traditional solvents, which can be described as molecular liquids, ionic liquids are composed of ions (see Figure 1.7 for the structures of the commonly used ionic liquids). Their unique properties such as non-volatility, non-flammability, and excellent chemical and thermal stability have made them an environmentally attractive alternative to conventional organic solvents. Ionic liquids have low melting points (<100 °C) and remain as liquids within a broad temperature window (<300 °C).

One of the most special properties for ionic liquids is their high polarity. On the normalized polarity scale (ENT) setting tetramethylsilane at 0.0 and water at 1.0, the polarity of common ionic liquids normally falls in the range of 0.6–0.7, similar to that of lower alcohols and formamide (Rantwijk, Lau & Sheldon, 2003). A correlation between the decrease in both the chain length of the alkyl substituents on the imidazolium ring of the cation and the anion size with an increase in polarity can be observed (Carmichael & Seddon, 2000). The polarity values of ionic liquids are sometimes sensitive to the temperature and the presence of water (Baker, S.N., Baker

G.A. & Bright, 2002). Because of the high polarity, ionic liquids present an ideal reaction melieu for chemical and biochemical reactions due to their ability to dissolve a wide range of different substances including polar and non-polar organic, inorganic, and polymeric compounds.

Despite of their high polarity, most of ionic liquids are hydrophobic and can dissolve up to 1% of water, and the presence of water may affect the physical properties of the ionic liquids (Seddon, Stark & Torres, 2000). However, the solubility of water in ionic liquids varies unpredictably (Rantwijk et al., 2003). For example, although 1-butyl-3-methylimidazolium tetrafluoroborate ([BMIm][BF_4]), 1-butyl-3-methylimidazolium hexafluorophosphate ([BMIm][PF_6]), and 1-butyl-3-methyl-imidazolium-bis-(trifluoromethylsulphonyl) imide ([BMIm][Tf_2N]) are similar on Reichardt's polarity scale, the former one is completely water-miscible while the latter two are only slightly soluble in water (Park & Kazlauskas, 2003).

Ionic liquids are generally immiscible with many organic solvents especially when the latter are nonpolar, such as hexane; whereas some may be miscible with polar solvents like dichloromethane and tetrahydrofuran (Park & Kazlauskas, 2003). The immiscibility of ionic liquids with either water or organic solvents has made them feasible to be used to form two-phase systems.

Compared to typical organic solvents, ionic liquids are much more viscous (35–500 cP viscosity for commonly used ionic liquids versus 0.6 cP for toluene and 0.9 cP for water at 25 °C) (Park & Kazlauskas, 2003; Brennecke & Maginn, 2001). The viscosity of an ionic liquid represents its tendency to form hydrogen bonding and the strength of its van der Waals interactions, and can be lowered by increasing the temperature or by adding some organic co-solvents. Normally, an ionic liquid with longer alkyl chains on the cation and a larger anion size presents a higher viscosity.

One obvious advantage of using ionic liquids over the use of normal organic solvents is that the physical and chemical properties of the ionic liquids, including their polarity, hydrophobicity, viscosity, and solvent miscibility, can be finely tuned

by altering the cation, anion, and attached substituents. This is important, because by manipulating the solvent properties, one is allowed to design an ionic liquid for specific reaction conditions, such as to increase the substrate solubility, to modify the enzyme selectivity, or to tailor the reaction rate.

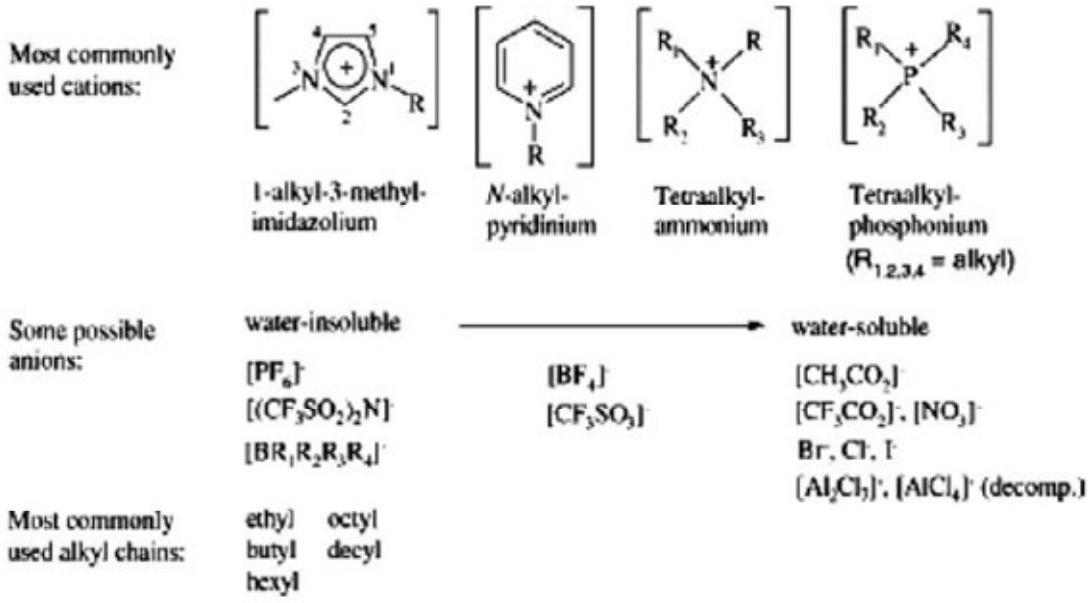

Figure 1.7 The building blocks of ionic liquids (taken from Yang & Pan, 2005).

CHAPTER TWO

EXPERIMENTAL METHOD AND INSTRUMENTATION

2.1 Commonly Used Reagents and Instrumentation

The polymer polyvinyl chloride (PVC) was high molecular weight and obtained from Fluka. The plasticiser, dioctyl phtalate (DOP) was 99 % from Aldrich. The additive potassium tetrakis (4-chlorophenyl) borate was selectophore, 98 % from Fluka. All solvents used in this thesis were of analytical grade and purchased from Merck, Johnson and Mathey, Acros, Fluka and Riedel. Solvents for the spectroscopic studies were used without further purification. The mercury sensitive dye of 4-{(1E, 3E)-3-[(4- chloro-phenyl)imino]-1-propenyl}-N,N-dimetilanilin (CPIPA) dye was supplied from Professor E. Çetinkaya and was synthesized in the laboratories of University of Ege. The other aluminum sensitive dye, N-N'-bis (2-hydroxybenzylidene)-ethane-1,2-diamine (Y1) was supplied from Associated Professor Dr. M.Y. Ergun and was synthesized in the organic laboratories of our department.

The metal ion solutions were prepared from their 0.1 M stock solutions by using the metal salts of $Hg_2(NO_3)_2$, $Hg(NO_3)_2$, and $Al(SO_4)_3.16H_2O$. N-N-Bis-(2-hydroxyethyl)-2-aminoethansulfonic acid (BES buffer) was from Merck. The preparation of buffer solutions was explained in Section 2.6.The commercial ionic liquid, 1-ethyl-3-methylimidazolium tetrafluoroborate (RTIL-III) was supplied from Fluka.

The heavy metal analysis studies were executed by fiber optical and flow system. The flow cell is made from polytetrafluoroethylene (PTFE) in the atelier of University of Ege. The flow system was explained in Section 2.2. pH measurements were recorded with a WTW pH meter. In all of the studies ultra pure water of Millipore was used.

Buffer components were of analytical grade (Merck and Fluka). For metal ion tests, **AAS** Standard solutions of Mn^{2+}, Hg^{2+}, Hg^{+}, Fe^{3+}, Al^{3+}, Cr^{3+}, Mn^{2+}, Mg^{2+}, Sn^{2+}, Cd^{2+}, Co^{2+}, Cu^{2+}, Ni^{+2}, Zn^{+2}, Bi^{+2} and Ca^{2+}(1000 mg/ L, Merck) were diluted with 0.01 M sodium acetate buffer of pH 5.0 and ultra pure water. Solutions of Hg^{+} and Hg^{2+} were prepared from the respective metal nitrates and diluted with 0.01 M sodium acetate buffer of pH 5.0. The pH values of the solutions were checked using a digital pH meter (WTW) calibrated with standard buffer solutions of Merck. All the experiments were carried out at room temperature; 25 ˚C. The synthesis of Y1 dye has been performed in our laboratories and published earlier. Schematic structure of the employed dye molecule is shown in Fig. 4.1.

Absorption spectra were recorded using a Shimadzu 1601 UV-Visible spectrophotometer. Steady state fluorescence emission and excitation spectra were measured using Varian Cary Eclipse Spectrofluorometer with a Xenon flash lamp as the light source. The fiber optic components were obtained from Varian and explained in detail in Section 2.1. The emission spectra were corrected using a piece of silica ground on both faces held in a triangular cuvette configuration called the diffuser. The heavy metal analysis studies were executed by fiber optical and flow system. The flow cell is made from polytetrafluoroethylene (PTFE) in the atelier of University of Ege. The flow system was explained in Section 2.3. pH measurements were recorded with a WTW pH meter. In all of the studies ultra pure water of Millipore was used.

2.2 Construction of Fiber Optical System

The fiber optical sensor was constructed with the commercial accessories of Varian Cary Eclipse Spectrofluorometer (Figure 2.1): Eclipse Fiber optic coupler, Fluorescence remote read probe (2 meters), Probe tip for solid measurements and Probe tips for liquid measurements (10 mm and 20 mm length tips). This method also allows the examination of samples remote from the instrument. The installation steps are:

- ***The fibre optic coupler*** is an accessory that enables the use of a fiber optic probe with Carry Eclipse spectrofluorometer. After the removal of the sample compartment of the Carry Eclipse, the fiber optic coupler was stabilized to the same position by the help of the screws.
- ***The fiber optic probe*** was connected to the coupler accessory by inserting the two connector ends into the two key holds.
- ***The probe tips*** were screwed onto the end of the probe. Due to the phase of the sample (solid or liquid), either a solid sample probe tip or a liquid sample probe tip were used.
- To ensure that the fiber optic system will operate at maximum performance, it is necessary to optimize the efficiency with which light passes through the coupling device before experimentation begins. The alignment was done by using the software of the instrument.

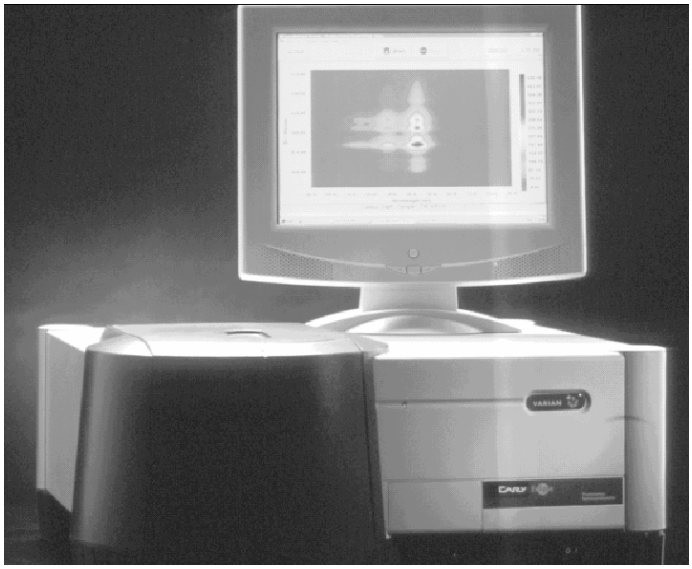

Fluorescence remote read probe

Fiber optic coupler accessory

probe tips

Figure 2.1 Varian Cary Eclipse Spectrofluoremeter and fiber optical system accessories.

2.3 Construction of the Sensing Films

The sensing cocktails were prepared due to the analyte type either with PVC or with various room temperature ionic liquids.

2.3.1 Cocktail and Thin Film Preparation Protocols

The membranes were prepared to contain the dye, PVC (High molecular weight), plasticizer (Dioctyl phthalate, DOP) and the additive potassium tetrakis-(4-chlorophenil) borate (PTCPB). The chemical structures of PVC, DOP and PTCPB were shown in Figure 2.3. The mixture was dissolved in the solvent of tetrahydrofuran (THF) and mixed by several hours by the help of a magnetic stirrer.

The resulting cocktail was spread on a 125 μm polyester support (Mylar from Du Pont) and dried in a desicator which was saturated with the solvent vapour. The polyester support was optically fully transparent, ion impermeable and exhibited good adhesion to PVC. The most important function of the polyester was to act as a mechanical support because the thin silicon films were impossible to handle. Once dried, the film was insoluble in water and could be cut into pieces of appropriate size. The approximate thickness of the film was 5 μm. Film thicknesses were measured using Tencor Alpha Step 500 Prophylometer. The films were kept in desiccators in the dark. This way, the photo stability of the membrane was ensured and the damage from the ambient air of the laboratory was avoided. For absorbance and steady state fluorescence measurements each sensing film was cut to 1.2 cm width and 2.5 cm length and fixed diagonally into the sample cuvette (Figure 2.2) and the absorption or emission spectra were recorded. For fiber optical and flow system measurements, each sensing film was cut to 1 cm width and 1 cm length and fixed into the flow cell shown in Figure 2.5.

The optode membranes were prepared to contain 120 mg of PVC, 240 mg of plasticizer (DOP), 1.17 mg of CPIPA dye(≈2.5 mmol dye kg−1 polymer), 1.49 mg of potassium tetrakis(4-chlorophenyl) borate and 1.5mL of THF. The amount of

potassium tetrakis(4-chlorophenyl) borate and the plasticizer type was optimized with some preliminary experiments. The resulting cocktails were spread onto a 125_m polyester support (Mylar TM type)in order to obtain the sensing films. The films were kept in a desiccator in order to avoid the damage from the ambient air of the laboratory. The film thicknesses of the sensing slides were measured with Tencor Alpha Step 500 prophylometer and found to be 6.12±0.071 μm. (Seiler & Simon, 1992; Bakker & Simon, 1992; Lerchi, Bakker, Rusterholz & Simon, 1992)

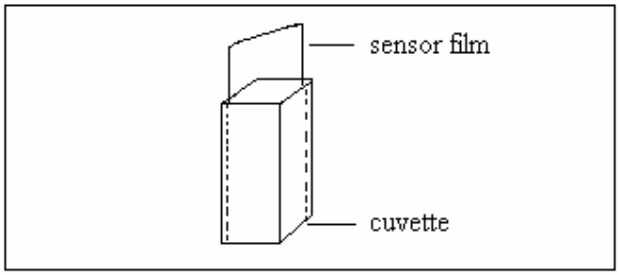

Figure 2.2 The placement of the sensor film in the sample cuvette.

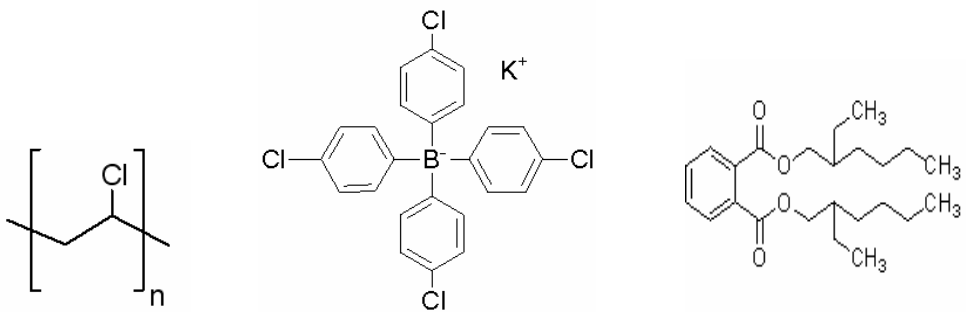

PVC PTCPB DOP

Figure 2.3 Structures of PVC, PTCPB and DOP.

2.4 Combination of The Flow System With Fiber Optic System (for metal ion determinations)

Metal response measurements were carried out with fiber optic probe (2m long) and solid sample tip accessories constructed on the spectrofluorometer. For instrumental control, data acquisition and processing the software package of the spectrofluorometer was used.

The tip of the bifurcated fiber optic probe was interfaced with a sensing film in a buffer containing 300 μL flow cell (Figure 2.5). The flow cell was equipped with a four channel Ismatec Reglo Analog peristaltic pump. Analyte solutions or buffers were transported by the peristaltic pump via tygon tubing of 2.06 mm i.d. (Figure 2.4)

Figure 2.4 Ismatec Reglo Analog peristaltic pump.

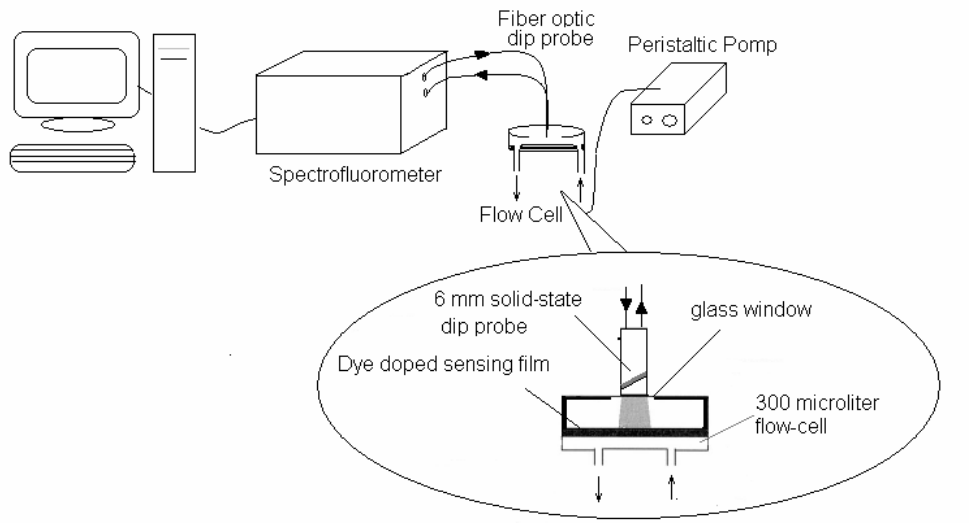

Figure 2.5 Instrumental set-up used for dye-doped thin film evaluation.

2.5 Photocharacterization of Studied Dyes

Photocharacterization studies of the employed dyes were performed with UV-Visible spectrophotometer and Spectrofluorometer either in steady stead or in time based mode. The spectrofluorometer was equipped with a Xenon flash lamp as the light source. The fiber optic components were obtained from Varian and explained in detail in Section 2.1. The emission spectra were corrected using a piece of silica ground on both faces held in a triangular cuvette configuration called the diffuser.

2.6 Quantum Yield Calculations

Fluorescence quantum yield values (Φ) of the employed dyes were calculated by using the comparative William's method (Williams, Winfield & Miller, 1983). This is a reliable method for recording Φ and involves the use of well characterized standard samples with known Φ values.

Essentially, solutions of the standard and test samples with identical absorbance at the same excitation wavelength can be assumed to be absorbing the same number of photons. Hence, a simple ratio of the integrated fluorescence intensities of the two solutions (recorded under identical conditions) will yield the ratio of the quantum

yield values. Since Φ for the standard sample is known, it is trivial to calculate the Φ for the test sample.

According to this method, the standard samples should be chosen to ensure they absorb at the excitation wavelength of choice for the test sample, and, if possible, emit in a similar region to the test sample. In order to minimize re-absorption effects (Dhami et al., 1995) absorbances in the 10 mm fluorescence cuvette should never exceed 0.1 at and above the excitation wavelength. Above this level, non-linear effects may be observed due to inner filter effects, and the resulting quantum yield values may be perturbed. This maximum allowable value of the recorded absorbance must be adjusted depending upon the path length of the absorption cuvette being used (for example, 10 mm = 0.1 maximum, 20 mm = 0.2 maximum etc).

In this study, standard 10 mm path length fluorescence and absorption cuvettes were used for running the fluorescence and absorbance measurements. The UV-vis absorption (absorbance≤0.10 at the excitation wavelength) and corrected fluorescence emission spectra were recorded for three or more solutions with increasing concentrations of the sample and the standard. The integrated fluorescence intensities (that is, the area of the fluorescence spectrum) were calculated from the fully corrected fluorescence spectrum. Graphs of integrated fluorescence intensity *vs* absorbance were plotted. The gradient of the plots were later used in the quantum yield calculations according to the following equation.

$$\theta_x = \theta_{st}\left(\frac{Grad_X}{Grad_{ST}}\right)\left(\frac{n_x^2}{n_{ST}^2}\right) \qquad (2.1)$$

Where the subscripts *ST* and *X* denote standard and test respectively, Φ is the fluorescence quantum yield, *Grad* the gradient from the plot of integrated fluorescence intensity *vs.* absorbance and n is the refractive index of the solvent.

2.7 Preparation of the Employed Buffer Solutions

2.7.1 Preparation of 0.05 M Acetic Acid/Acetate Buffer

0.102 g of acetic acid and 0.2624 g of sodium acetate were dissolved in 950 mL ultra pure water. The solution was titrated to pH 5.0 at the lab temperature of 20^{o}C either with 0.1 M HNO_3 or 0.1 M NaOH as needed. The resulting solution was made up to 1000 ml with ultra pure water in a volumetric flask. The buffer solutions in the range of pH 3.0-7.0 were prepared by the same way by adjusting to the desired pH.

2.7.2 Preparation of 0.05 M Acetic Acid/Acetate Buffer in the Physiological Salinity Level

0.09 g of acetic acid and 0.2788 g of sodium acetate were dissolved in 950 mL ultra pure water. 7.699 g of NaCl was added to this solution. The solution was titrated to pH 5.0 at the lab temperature of 20^{o}C either with 0.1 M HNO_3 or 0.1 M NaOH as needed. After, it was made up to 1000 ml with ultra pure water in a volumetric flask. The resulting solution was in the physiological salinity level containing 135 mM NaCl (The ionic strength of the solution was 135 mM). The buffer solutions in the range of pH 3.0-6.0 were prepared by the same way by adjusting to the desired pH.

2.7.3 Preparation of 0.05/0.01 M NaH_2PO_4/Na_2HPO_4 Buffer

0.348/0.696 g of NaH_2PO_4 and 0.284/0.5822 g of Na_2HPO_4 were dissolved in 950 mL ultra pure water. The solution was titrated to pH 7.0 at the lab. temperature of 20 ^{o}C either with 0.1 M HNO_3 or 0.1 M NaOH as needed. The resulting solution was made up to 1000 ml with ultra pure water in a volumetric flask. The buffer solutions in the range of pH 7.0-9.0 were prepared by the same way
by adjusting to the desired pH.

2.7.4 Preparation of 0.05 M BES Buffer

1.176 g of BES sodium salt (N,N-Bis(2-hydroxyethyl)-2-aminoethanesulfonic acid sodium salt, MW = 235.2 g, pKa of free acid = 7.1) was dissolved in approx. 950ml of ultra pure water. The solution was titrated to pH 7.0 at the lab temperature of 20 ^{o}C either with 0.1 M HNO_3 or 0.1 M NaOH as needed. The resulting solution was made up to 1000 ml with ultra pure water in a volumetric flask. The buffer solutions in the range of pH 5.0-7.0 were prepared by the same way by adjusting to the desired pH.

CHAPTER THREE

PHOTOCHARACTERIZATION OF CHLORO PHENYL IMINO PROPENYL ANILINE DYE FOR SELECTIVE HG (II) SENSING

3.1 Introduction

Mercury is a compound that can be found naturally in the environment. It can be found in metal form, as mercury salts or as organic mercury compounds.

Mercury enters the environment as a result of normal breakdown of minerals in rocks and soil through exposure to wind and water. Release of mercury from natural sources has remained fairly the same over the years. Still mercury concentrations in the environment are increasing; this is ascribed to human activity.

Most of the mercury released from human activities is released into air, through fossil fuel combustion, mining, smelting and solid waste combustion. Some forms of human activity release mercury directly into soil or water, for instance the application of agricultural fertilizers and industrial wastewater disposal. All mercury that is released in the environment will eventually end up in soils or surface waters.

Mercury is not naturally found in foodstuffs, but it may turn up in food as it can be spread within food chains by smaller organisms that are consumed by humans, for instance through fish. Mercury concentrations in fish usually greatly exceed the concentrations in the water they live in. Cattle breeding products can also contain eminent quantities of mercury. Mercury is not commonly found in plant products, but it can enter human bodies through vegetables and other crops, when sprays that contain mercury are applied in agriculture.

Mercury from soils can accumulate in mushrooms. Acidic surface waters can contain significant amounts of mercury. When the pH values are between five and seven, the mercury concentrations in the water will increase due to mobilization of mercury in the ground. Once mercury has reached surface waters or soils microorganisms can convert it to methyl mercury, a substance that can be absorbed

quickly by most organisms and is known to cause nerve damage. Fish are organisms that absorb great amounts of methyl mercury from surface waters every day. As a consequence, methyl mercury can accumulate in fish and in the food chains that they are part of. (taken from http://www.lenntech.com/periodic-chart-elements/hg-en.htm)

Mercury has a number of effects on humans that can all of them be simplified into the following main effects:

- Disruption of the nervous system
- Damage to brain functions
- DNA damage and chromosomal damage
- Allergic reactions, resulting in skin rashes, tiredness and headaches
- Negative reproductive effects, such as sperm damage, birth defects and miscarriages

Owing to the toxic effects, Hg (II) has been one of the most important cations in analytical and environmental chemistry. Different dyes have been used for spectral Hg (II) detection either in immobilized or free form. Certain porphyrins or neutral ionophores such as dithiocarbamates were employed in immobilized form. Porphyrin based sensors suffer from lack of selectivity to Hg (II) over other heavy metals, such as Ag (I), Cd (II) and Pb. The enzyme inhibition effect of mercury on immobilized horseradish peroxidase and urease was also utilized to develop the optical sensors for Hg (II). Murkovic et. al. used a lipophilic borate salt as a reagent for Hg (II), along with an amphiphilic carbocyanine dye as the optical transducer in plasticized PVC . They reported 30 min response time for 100 nM concentration levels.

Akkaya et.al offered bis(2-pyridyl)-substituted boratriazaindacene dye as an NIR-emitting chemosensor for Hg (II). They performed their measurements in acetonitrile for 1-20 μM concentration range of Hg (II). Recently Huang et. al. used highly fluorescent Rhodamine B molecules together with gold-nanoparticles (AuNP) for detecting Hg (II) ions in aqueous solutions. They improved the selectivity of the probe by modifying the AuNP surfaces with thiol ligands (mercaptopropionic acid, mercaptosuccinic acid, and homocystine) and adding a chelating ligand (2,6-

pyridinedicarboxylic acid) to the sample solutions. Coskun and Akkaya reported a solution phase ratiometric fluorescent chemosensor for Hg (II) employing a boradiazaindacene dye for the concentration range of 0-25 μM Hg^{2+}.

Here we present application of the long wavelength excitable fluorophore; chloro phenyl imino propenyl aniline (CPIPA) in selective Hg^{2+} sensing. Its possible use for optical sensing of Hg^{2+} and typical sensor characteristics such as working range, sensitivity, limit of detection, and selectivity has been investigated.

3.2 Experimental

3.2.1 Materials

The polymer membrane components, polyvinyl chloride (PVC) (high molecular weight) potassium tetrakis-(Cchlorophenyl) borate (PTCPB), and the plasticizer, bis-(2-ethylhexyl) phthalate (DOP), were obtained from Fluka. Absolute ethanol, THF and hydrochloric acid (HCl) were of analytical grade. Solvents for the spectroscopic studies were used without further purification.

Solutions of Hg^{+} and Hg^{2+} were prepared from the respective metal nitrates and diluted with 0.01 M sodium acetate buffer of pH 5.0. The pH values of the solutions were checked using a digital pH meter (WTW) calibrated with standard buffer solutions of Merck. All the experiments were carried out at room temperature; 25 ˚C. The synthesis of CPIPA dye has been performed in our laboratories and published earlier. Schematic structure of the employed dye molecule is shown in Fig. 3.1.

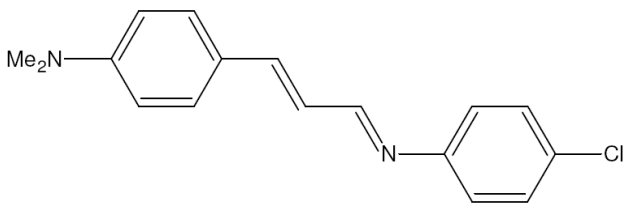

Figure 3.1 4-{(1E, 3E)-3-[(4-klorophenyl)imino]-1-prophenyl}-N,N-dimethylaniline (CPIPA).

3.2.2. Instrumentation

Absorption spectra were recorded using a Shimadzu 1601 UV-Visible spectrophotometer. Steady state fluorescence emission and excitation spectra were measured using Varian Cary Eclipse Spectrofluorometer with a Xenon flash lamp as the light source. pH measurements were recorded with a WTW pH meter. In all of the studies, ultra pure water of Millipore was used.

3.3 Result and Discussion

3.3.1 Spectral Response of the CPIPA Dye

Spectral characterization data of CPIPA in the solvents of EtOH, DCM, THF and in solid matrix of PVC was published earlier (Derinkuyu, 2007).

The dye exhibited high molar extinction coefficients and quantum yield values in the employed matrices (ε=50300M $^{-1}$ cm^{-1} ($\lambda_{max\ 1}$: 400 nm in EtOH), ε_1=28000 M $^{-1}$ cm^{-1} and ε_2=56000 M $^{-1}$ cm^{-1} ($\lambda_{max\ 1}$: 389 nm, $\lambda_{max\ 2}$: 547 nm in PVC)). The quantum yield in PVC matrix is 0.37 for the CPIPA dye in reference to Rose Bengal (Derinkuyu, 2007). The p*K*a value of 10.25 makes the CPIPA dye stable in the acidic and near neutral region of the pH scale. These promising spectral characteristics of the dye encouraged us to use the CPIPA for Hg (II) sensing purposes.

Table 3.1 Table 4.1 Spectral characterization of CPIPA dye (λ^{ex}_{max} : excitation wavelength in nm, λ^{em}_{max} : emission wavelength in nm, $\Delta\lambda_{ST}$: Stoke's shift and θ_F : Quantum yield)

Compound	Solvent/Matrix	λ^{ex}_{max}	λ^{em}_{max}	$\Delta\lambda_{ST}$ (Stoke's shift)	θ_F (Quantum Yield)
CPIPA	EtOH	504	420	84	0,00694 in DCM
CPIPA	DCM	460	385	75	
CPIPA	THF	479	420	59	
CPIPA	To:EtOH	478	395	83	
CPIPA	PVC	593	556	37	0,37400

3.3.2 pH Optimization Studies

The pH dependency of the CPIPA dye upon interaction with Hg (I) and Hg (II) was investigated at fixed Hg (I) or Hg (II) concentrations ([Hg (I) or Hg (II)] = 10^{-3} M) in the pH range of 4.0–7.0. The steady state fluorescence emission spectra of PVC-doped CPIPA were recorded before and after exposure to 10^{-3} M buffered Hg^{+} and Hg^{2+} solutions at different pH values. Solutions of pH 4.0-5.0 and 6.0 were prepared in 5.10^{-2} M acetic acid/acetate buffer. The pH 7.0 solution was prepared with BES; sodium salt of (N,N-Bis(2-hydroxyethyl)-2-aminoethanesulfonic acid) (MW = 235.2 g, pKa of free acid = 7.1).

The steady state fluorescence emission spectra of PVC-doped CPIPA recorded before and after exposure to Hg(I) and Hg(II) solutions at different pH values. The results are shown throughout Fig. 3.2 and Fig. 3.9.

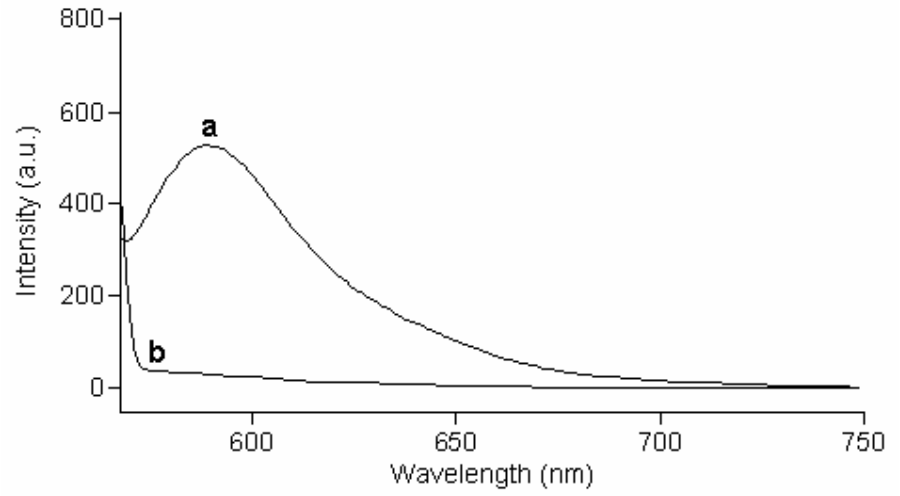

Figure 3.2 Response of the PVC doped CPIPA dye to Hg (I) in BES buffer at pH=7.0 (a: initial, b: after exposure to 10^{-3} M buffered Hg^{+} solution)

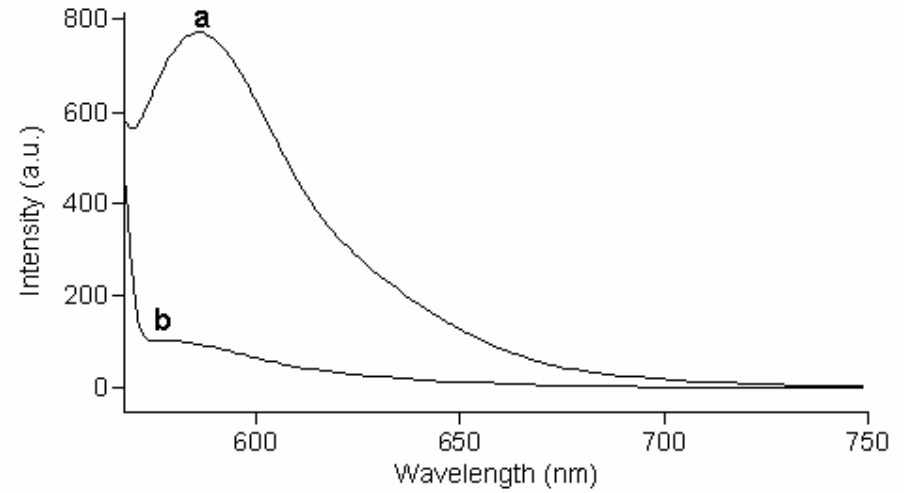

Figure 3.3 Response of the PVC doped CPIPA dye to Hg (I) in acetic acid/acetate buffer at pH=6.0 (a: initial, b: after exposure to 10^{-3} M buffered Hg^{+} solution).

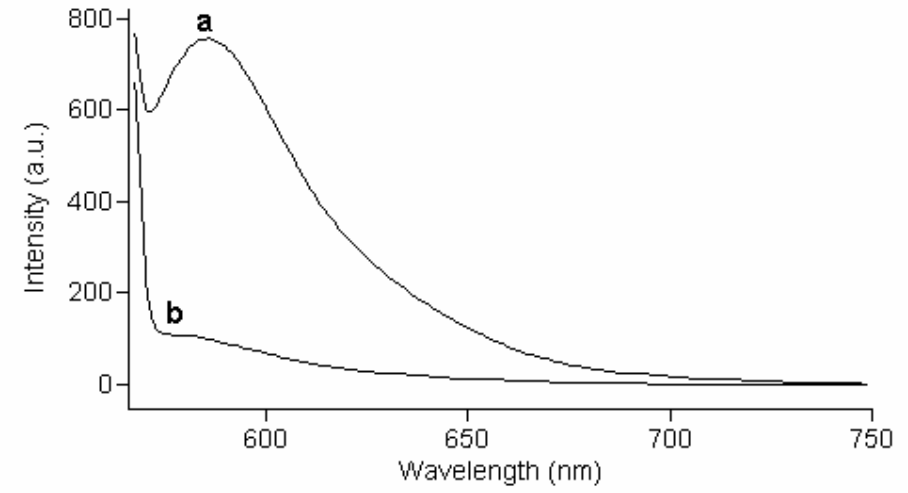

Figure 3.4 Response of the PVC doped CPIPA dye to Hg (I) in acetic acid/acetate buffer at pH=5.0 (a: initial, b: after exposure to 10^{-3} M buffered Hg^{+} solution).

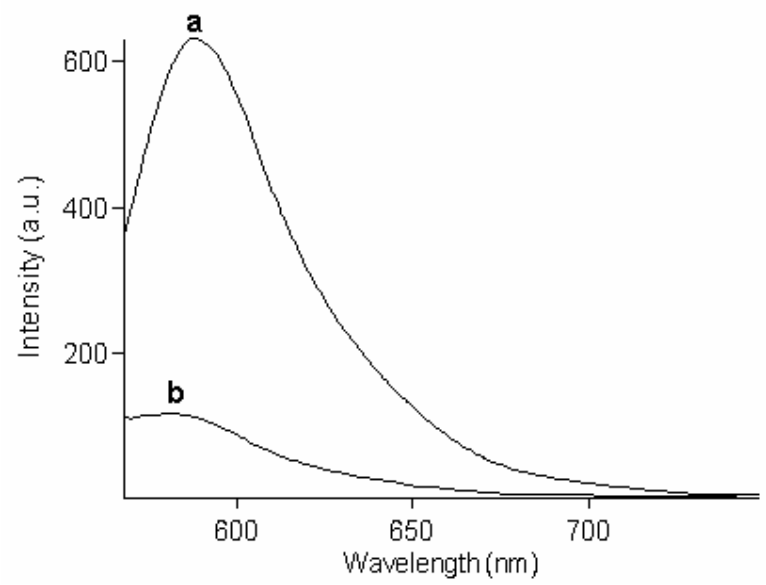

Figure 3.5 Response of the PVC doped CPIPA dye to Hg (I) in acetic acid/acetate buffer at pH=4.0 (a: initial, b: after exposure to 10^{-3} M buffered Hg^{+} solution).

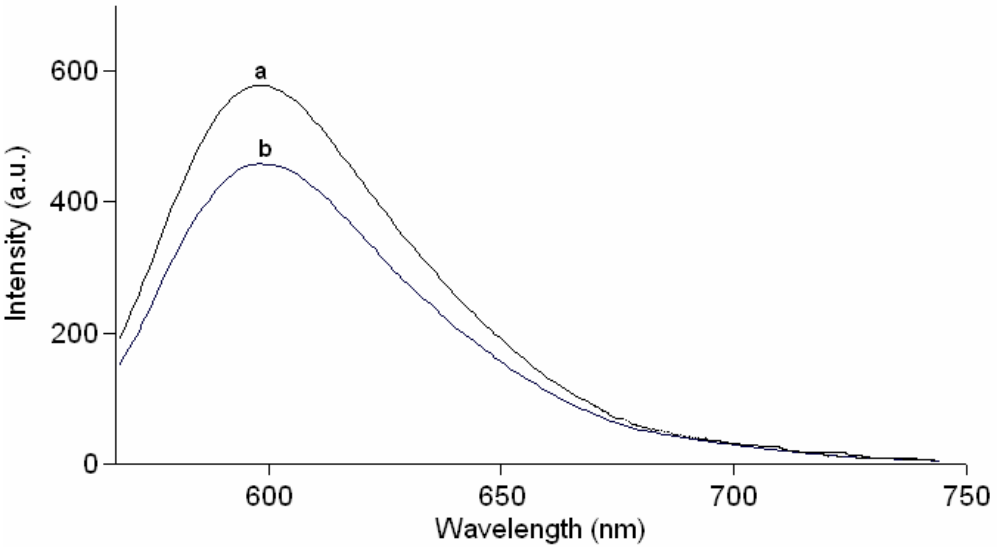

Figure 3.6 Response of the PVC doped CPIPA dye to Hg (II) in BES buffer at pH=7.0 (a: initial, b: after exposure to 10^{-3} M buffered Hg^{2+} solution).

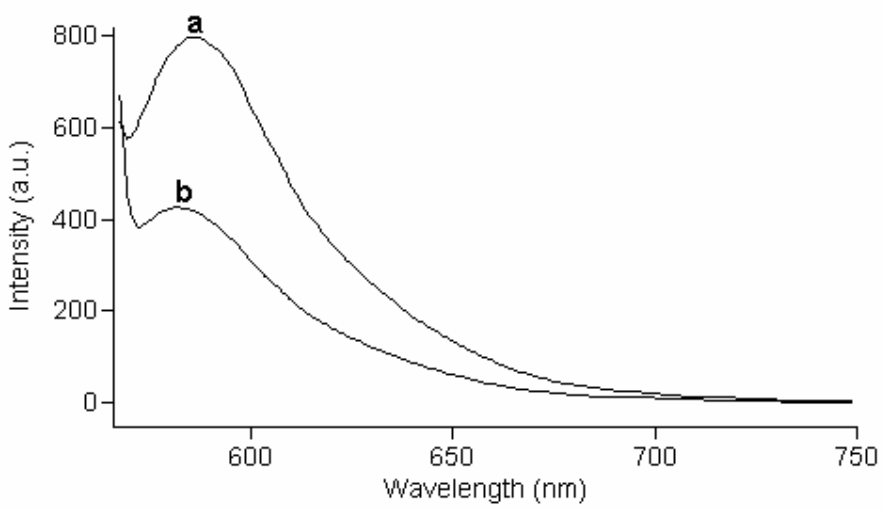

Figure 3.7 Response of the PVC doped CPIPA dye to Hg (II) in acetic acid/acetate buffer at pH=6.0 (a: initial, b: after exposure to 10^{-3} M buffered Hg^{2+} solution).

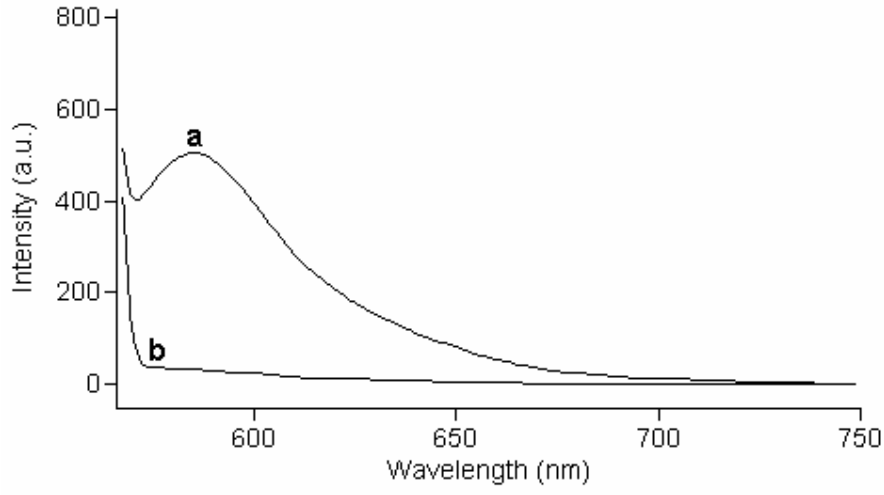

Figure 3.8 Response of the PVC doped CPIPA dye to Hg (II) in acetic acid/acetate buffer at pH= 5.0 (a: initial, b: after exposure to 10^{-3} M buffered Hg^{2+} solution)

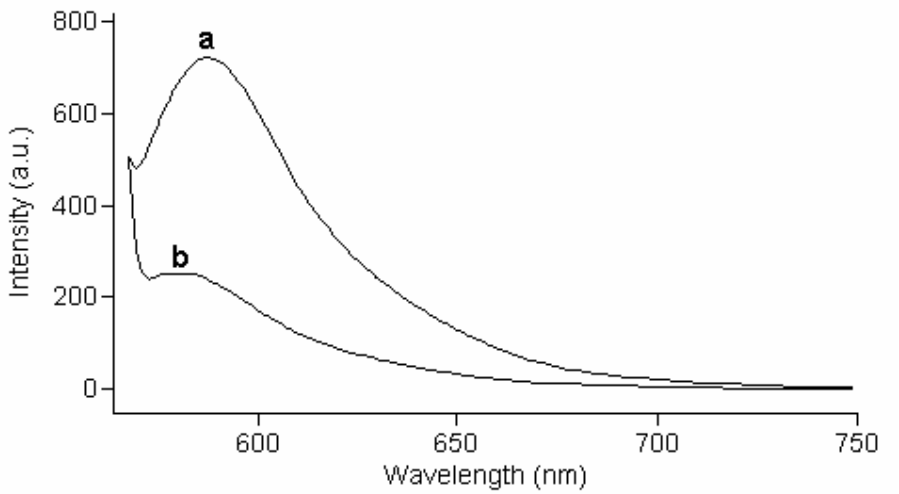

Figure 3.9 Response of the PVC doped CPIPA dye to Hg (II) in acetic acid/acetate buffer at pH= 4.0 (a: initial, b: after exposure to 10^{-3} M buffered Hg^{2+} solution).

Optimum conditions of pH were investigated separately at constant concentrations of Hg (I) or Hg (II) ions. The analytical signal (I_0–I/I_0) produced by the Hg (II) ions was optimum at the pH of 6.0 (see Fig. 3.10). Therefore, pH 4.0 - 6.0 was chosen as the optimum pH range for Hg (II) determination.

A selectivity comparison of Hg (I) over Hg (II) in separate solutions at different pH values was investigated. From Figure 3.2 to Figure 3.9 it can be concluded that, the CPIPA dye was affect in selective binding of both Hg (I) and Hg (II) with respect to other possible interferants. However, speciation is not possible.

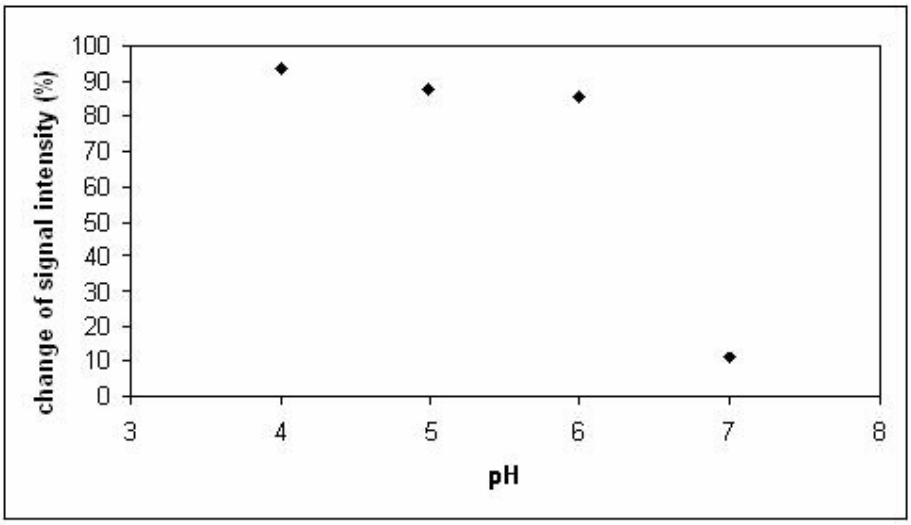

Figure 3.10 Upon exposure to fixed concentrations of Hg (II), the membrane response to different pH values.

Figure 3.11 and 3.12 reveal signal response of PVC doped CPIPA upon exposure to mercury concentrations from 1.0×10^{-9} to 3.0×10^{-5} M, at pH 6.0 and 4.0 respectively. The membrane exhibited 83% and 69% relative signal changes at pH 6.0 and 4.0 in direction of decrease in fluorescence intensity.

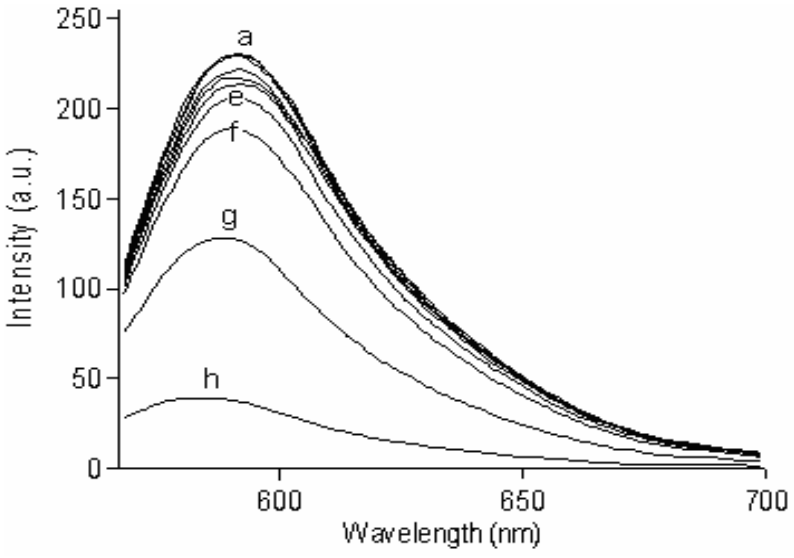

Figure 3.11 Emission based response of the CPIPA doped PVC membrane to different concentrations of Hg (II) at pH=6.0 (a: Hg (II) free buffer, b: 10^{-9}, c: 10^{-8}, d: 10^{-7}, e: 10^{-6}, f: 10^{-5}, g: 2.10^{-5}, h: 3.10^{-5} M, relative signal change 83%).

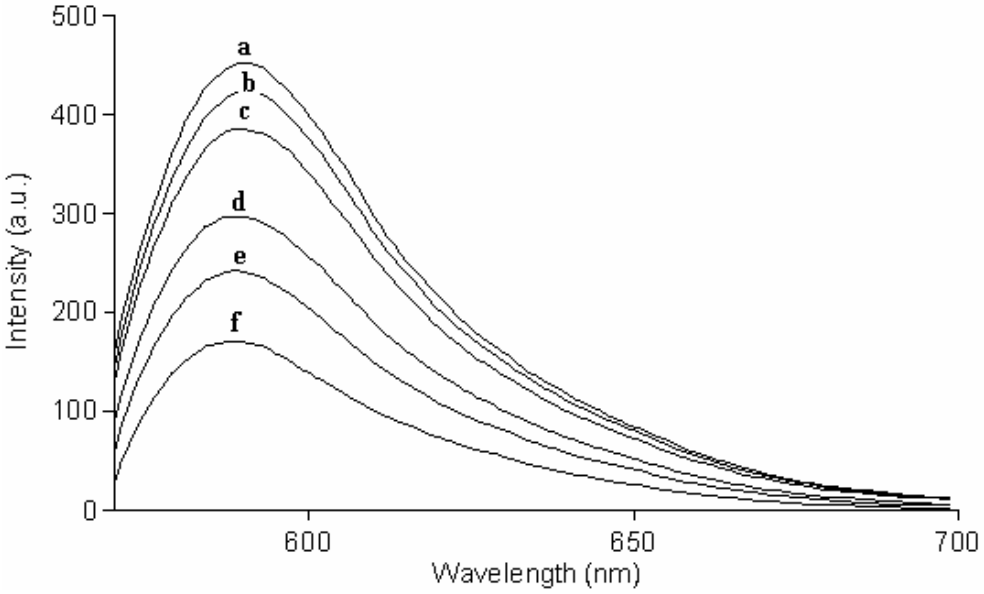

Figure 3.12 Emission based response of the CPIPA doped PVC membrane to different concentrations of Hg (II) at pH=4.0 (a: buffer, b: 10^{-9}, c: 10^{-8}, d: 10^{-7}, e: 10^{-6}, f: 10^{-5}, g: 2.10^{-5}, h: 3.10^{-5} M, relative signal change 69%).

Figure 3.13 reveals calibration plot of membrane at pH 4.0. Linearity of the calibration plot of membrane at pH 4.0 was better than that of obtained at pH 6.0. For this reason the pH 4.0 was chosen as working pH for further studies.

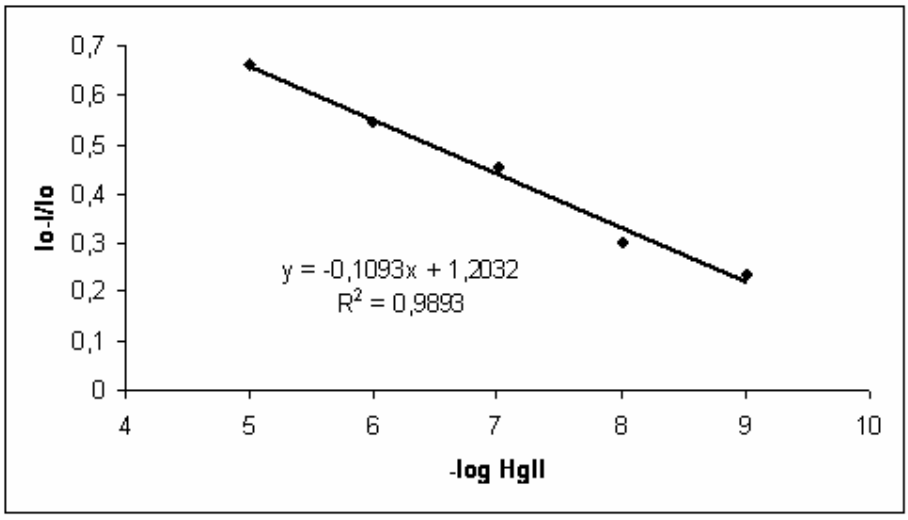

Figure 3.13 Normalized fluorescence intensities vs. Hg (II) concentration for CPIPA doped PVC membrane at pH=4.0.

3.3.3 Effect of Salinity

The mercury concentration–dependent spectral response of sensor membrane was investigated at pH 4.0.

Response of the sensor membrane was tested by making the ionic strength of the buffer solution 135 mM with NaCl. The relative signal change of the emission spectrum of the sensor in contact with this solution was dropped from 69 % to 50 %.

Emission based spectral response and calibration curve of the membrane in BES-buffered and 135 mM NaCl–containing solutions at pH 4.0 were shown in Figure 3.14.

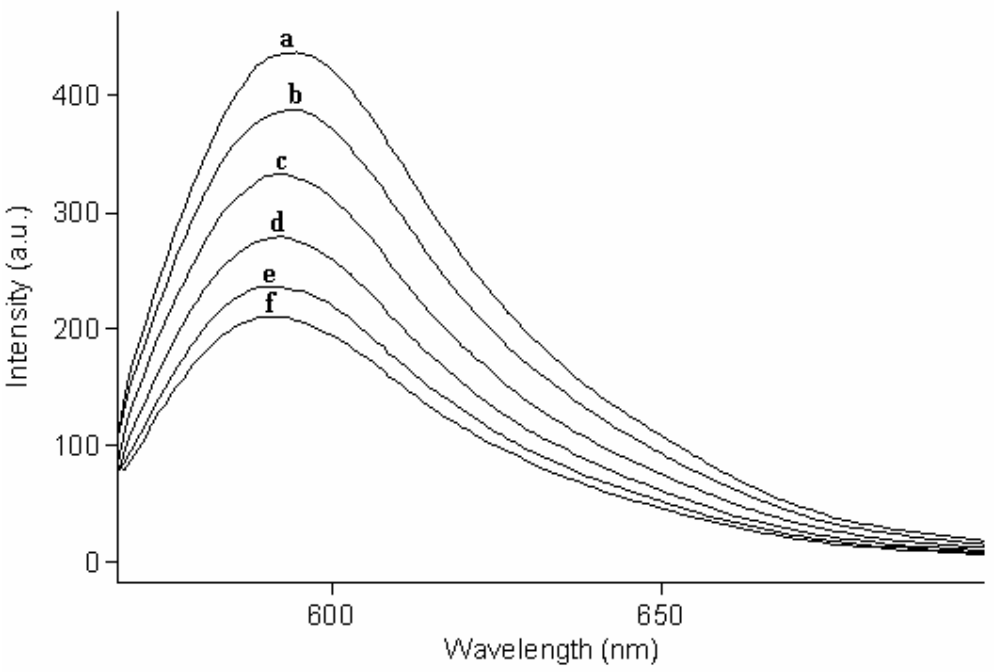

Figure 3.14 Emission based response of the CPIPA doped PVC membrane to different concentrations of Hg (II) at pH=4.0 in presence of 135 mM NaCl (a: buffer + NaCl, b: 10^{-9}, c: 10^{-8}, d: 10^{-7}, e: 10^{-6}, f: 10^{-5} M NaCl containing Hg (II) solutions, relative signal change 50%).

3.3.4 Complex Formation Between CPIPA Dye and Hg(II)

Concentration dependent changes in the absorption spectrum of CPIPA in ethanol after exposure to Hg (I) and Hg (II) are shown in Figure 3.15 and Figure 3.16. After addition of Hg (II), an isobestic point at 340 nm was observed. In case of Hg (I) no isobestic point was observed in the spectra. An increasing absorbance peak appeared at 284 nm is the evidence of complex formation between Hg (II) and CPIPA (See Fig 3.16). Upon exposure to Hg (I) the increasing absorption band at 284 nm was disappeared (See Fig 3.15). However in case of Hg (II), a strong hypochromic effect was observed for the bands of 260 nm and 400nm.

This substantial bathochromic shift and accompanying isobestic point formation observed in case of Hg(II) can be attributed to the real ground-state complex formation with Hg(II) cations.

Information on the stoichiometry of the complex was obtained from the continuous variation method (Job's method). In Job's method different amounts of stock solutions of metal and ligand are mixed varying the mole ratio of reactants. The principle of the method is as follows: the absorbance (Abs) is measured for a series of solutions containing the ligand and the cation such that the sum of the total concentrations of ligand and cation is constant:

$$C_L + C_M = C \text{ (constant)}$$

The position of the maximum of absorbance (Abs_{max}) is then related to the ratio *m*/*l*, as shown below (Gunduz, 2002).

$$X = \frac{C_M}{C_M + C_L}$$

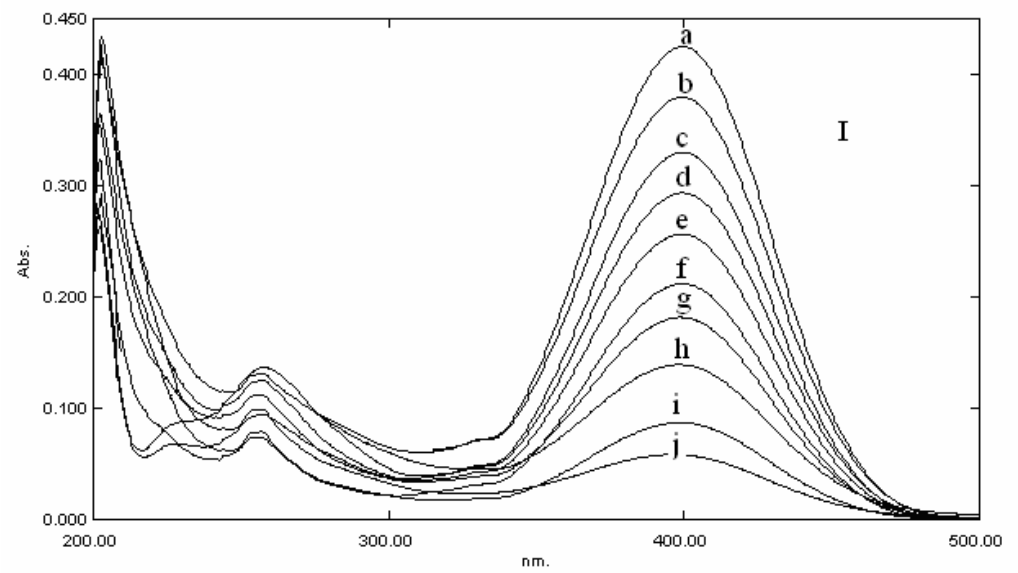

Figure 3.15 Changes in the absorption spectra during the complex formation of CPIPA dye (1 × 10−5 mol l^{-1}), with the Hg (I) ions in ethanol. a: CPIPA dye solution, b: 1×10^{-6}M Hg^{+}, c: 2×10^{-6}M Hg^{+}, d: 3×10^{-6}M Hg^{+}, e: 4×10^{-6}M Hg^{+}, f: 5×10^{-6}M Hg^{+}, g: 6×10^{-6}M Hg^{+}, h: 7×10^{-6}M Hg^{+}, i:8×10^{-6}M Hg^{+}, j:9×10^{-6}M Hg^{+}.

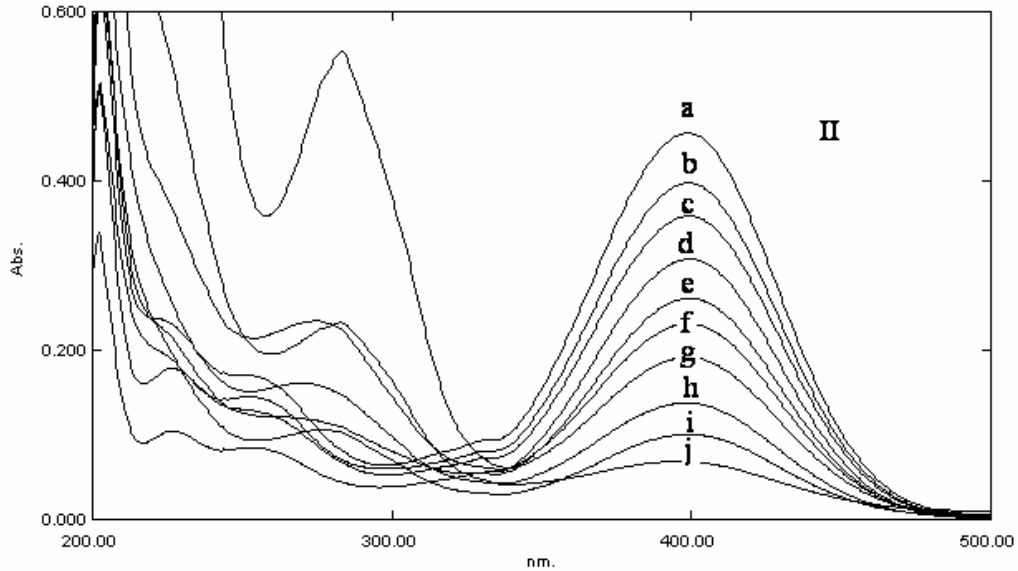

Figure 3.16 Changes in the absorption spectra during the complex formation of CPIPA dye (1 × 10−5 mol l^{-1}), with the Hg (II) ions in ethanol. a: CPIPA dye solution, b: 1×10^{-6}M Hg^{2+}, c: 2×10^{-6}M Hg^{2+}, d: 3×10^{-6}M Hg^{2+}, e: 4×10^{-6}M Hg^{2+}, f: 5×10^{-6}M Hg^{2+}, g: 6×10^{-6}M Hg^{2+}, h: 7×10^{-6}M Hg^{2+}, i:8×10^{-6}M Hg^{2+}, j:9×10^{-6}M Hg^{2+}.

Figure 3.17; Job's plot for the employed dye and metal; reveals complex formation between CPIPA and Hg^{2+} in ethanol. From the Job's plot for Hg (II) stoichiometry of the metal–ligand complex of Hg (II) -CPIPA was found to be 1:1 at the employed total concentration; 1×10^{-5} mol l^{-1}.

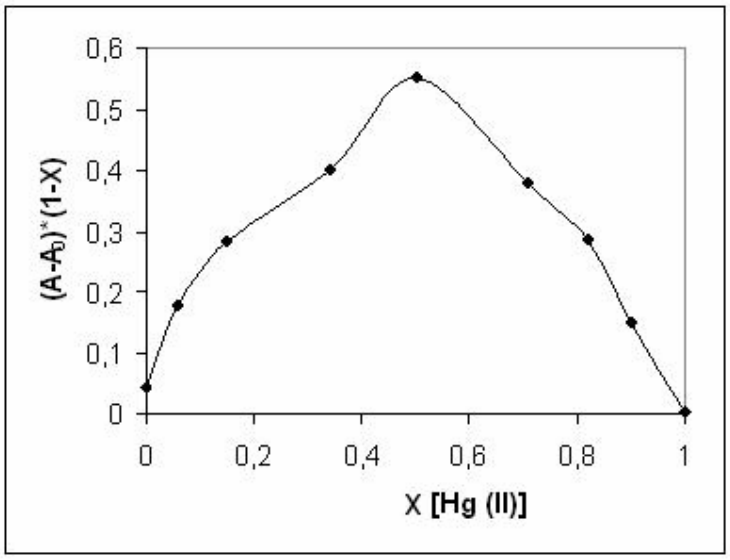

Figure 3.17 Job's plot for complex formation of CPIPA with Hg^{2+} in ethanol (λabs = 396 nm, *C*sum = 1×10^{-5} M). Absorption based data was extracted from short-wavelength maximum of the absorption spectra of Hg^{2+} complex.

3.3.4.1Mecanism of Quenching

The CPIPA dye is supposed to form a non-fluorescent complex with Hg (II) and statically quenched in ground state. According to the theory, the steady-state absorption spectrum of the chromophore is expected to be perturbed in the presence of quencher that interacts with the chromophore in the ground state. For this reason the nature of the ground state was investigated by studying the molecule's steady state absorption spectrum (See Fig. 3.18). Curves from a to k are the absorption spectra of the CPIPA dye in EtOH in absence and presence of the quencher. Absorption spectra of the CPIPA dye in EtOH solution exhibits an appreciable decrease in the intensity and conformational change after exposure to certain volumes of 10^{-5}M quencher (curves from a to k).The absorption curves of CPIPA dye exhibited significant spectral shift in the absorption maxima having an isobestic

point at 340 nm. This observation reveals the possibility of the formation of a ground state complex between the CPIPA dye and Hg (II) and therefore the quenching is of static type.

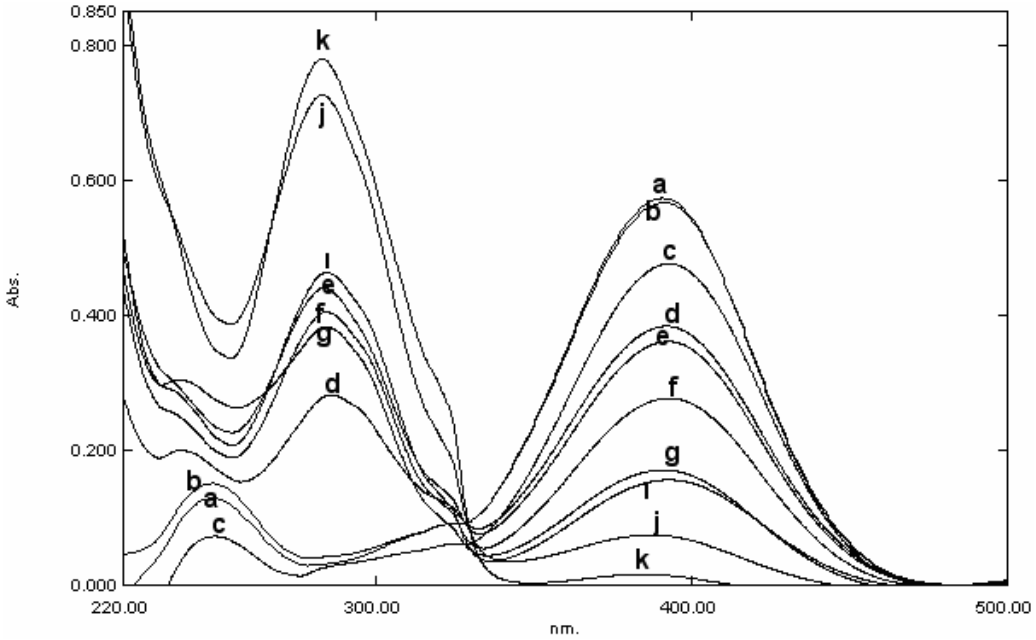

Figure 3.18 Absorption spectra of CPIPA in EtOH after addition of certain amounts of Hg (II) solutions a) CPIPA in EtOH, b) 0,3 ml of 1.0 x 10^{-5} M Hg (II) solution, c) 0,6 ml Hg (II) d) 0,9 ml Hg (II) e) 1,2 ml Hg (II) f) 1,5 ml Hg (II) g) 1,8 ml Hg (II) ı) 2,1 ml Hg (II) j) 2,4 ml Hg (II) k) 2,7 ml Hg (II)

3.3.4.2 Selectivity Studies

The dye-doped membrane exhibited remarkable fluorescence intensity quenching upon exposure to Hg (II) ions at pH 6.0. The effects of the Fe^{2+} and other responding ions (Cu^{2+}, Ca^{2+},Hg^{+}, Pb^{2+}, Al^{3+}, Cr^{3+},Mn^{2+},Mg^{2+}, Sn^{2+}, Cd^{2+}, Co^{2+} and Ni^{2+}) were negligible. Results of these tests were published earlier (Derinkuyu, 2007)

3.3.5 Time Based Data Acquisition

The time based response data of the sensor membrane for the determination of Hg (II) was acquired in the concentration range from 10^{-9} to 10^{-5}M (see Fig. 3.19). The sensor was not reversible within the working range.

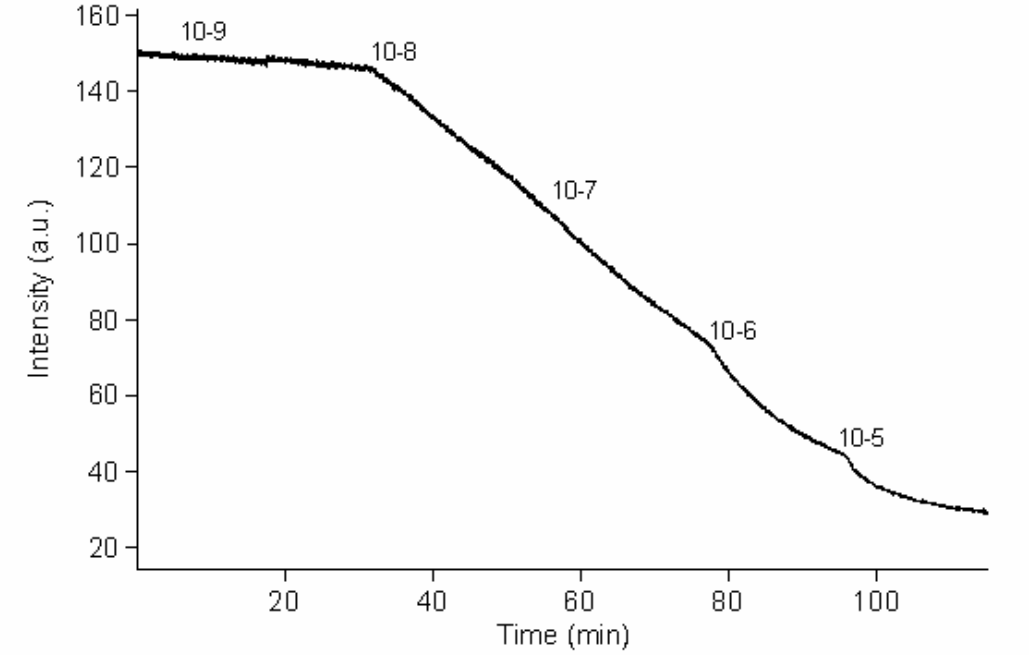

Figure 3.19 Time dependent response of the sensor membrane after introduction of certain concentrations of Hg (II) solutions to the flow system.

From Fig. 3.19 it can be concluded that limit of quantification of the employed dye is between $1x10^{-8}$ -$1x10^{-5}$ M.

3.4 Conclusion

In this chapter original Hg(II) sensor was tried to be developed by making use of 4-{ (1E, 3E)-3-[(4- chloro-phenyl)imino]-1-propenyl}-N,N-dimetilanilin (CPIPA), a newly synthesized indicator dye. CPIPA, was spectrophotometrically characterized in various solvents and ionic liquids. Spectral response of dye to dissolved mercury and pH and was investigated in to dept. The complex stoichiometry between dye and

heavy metal was defined with Job's Method. In addition to that, the transformation of spectral response by time was studied. The indicator dye CPIPA exhibited relative signal change extending to 83% when immobilized in PVC matrix. The work described here demonstrates a selective fluorescence based molecular probe for Hg (II) ions. To our knowledge the CPIPA dye was used for the first time as a fluoroionophore in the optical mercury sensor design. The quantum yield of the dye in PVC is reasonably high (0.37) and could be excited at 556 nm with commercially available cheap LEDs. The sensor can be used at pH 4.0 for quantitative determination of Hg^{2+} in the concentration range of 1.0×10^{-9} to 3.0×10^{-5} M. A quite good LOD (4.3 ppb) was reached.

CHAPTER FOUR

SELECTIVE DETERMINATION OF ALUMINIUM WITH N-N'-BIS (2-HYDROXYBENZYLIDENE)-ETHANE-1,2-DIAMINE BY SPECTROFLUORIMETRIC METHOD

4.1 Introduction

Natural aluminum occurs in the soil and makes up about 8 % of the surface of the earth. Higher concentrations may exists in soil surrounding waste sites associated with certain industries such as coal combustion and aluminum mining and smelting (U.S. Public Health Service, 1992, p. 67). Flux of dust from ores and rock materials are the largest source of particle-borne aluminum (Lee and von Lehmden, 1973; Sorrenson *et al.*, 1974). Both natural processes (weathering of aluminosilicate crystal material) and human activities (mining and agriculture) continually add dust particles to the environment (Eisenrich,1980; Filipek *et al.*, 1987).

In the atmosphere, aluminum is mainly found as aluminosilicates associated with particulate matter and the background levels of aluminum in the atmosphere generally range from 0.005 to 0.18 mg/m^3 (Sorrenson *et al.*, 1974). Aluminum concentrations in natural water normally are small but are found to be higher in the urban areas (Constantini and Giordano, 1991). The increasing amount of aluminum is being leached continuously by acid rain (Harris *et al.*, 1996) and contributes significantly to environmental inputs. Worldwide, it has been estimated that 40 % of arable soils and perhaps as much as 70 % of lands that can be cultivated are acidic enough to have an aluminum toxicity problem (World Food Nutrition Study, 1977).

Many types of foods contain aluminum because they are grown in soil that contains aluminum. When the soil pH is lower than 4.5-5.0, aluminum is solubilized in the soil water and absorbed by plant roots (Matsumoto, 2000). Apart from this, food additives also contribute substantial amounts of aluminum in the diet. Aluminum is present in many manufactured foods and is added to drinking water for

purification purposes (Levesque *et al.*, 2000). The common foods with aluminum-containing food additives include some processed cheese, baking powders, cake mixes, etc. The average concentration of aluminum in cola drinks was found to be 0.1 mg/g. Dry tea leaves have 555-1009 μg/g aluminum and typical infusion has 4.5-6.0 μg/ml aluminum. Infusion of coffee has an aluminum concentration 0.04-0.30 μg/ml (Koch *et al.*, 1988).

Aluminum absorption seems to be very low, but many factors can enhance it in animals and humans (Deng *et al.*, 1998). One of the significant routes of aluminum absorption is through the gut (Ittel, 1993). Aluminum is clearly a powerful neurotoxicant. Considerable evidence exists that aluminum may play a role in the aetiology or pathogenesis of Alzheimer's disease, but whether the link is casuals is still open to debate (Flaten, 2001).

Many nonsoluble aluminum compounds could pass into their ionic state under acidic conditions. Andropogenic activities like refineries, mineral mining, the usage of aluminum-based coagulants and many other reasons increase the dissolved Al (III) levels. Owing to the toxic effects, Al (III) has been one of the most important cations in biomedical analytical and environmental chemistry. Al^{3+} ions exert several neurotoxic effects. It has been suspected that aluminum may be an important cause of Alzheimer's disease, bone softening and severe toxic effect to patients with chronic renal failure (Flaten, 2001, Aksuner, 2008).

Morin (3,5,7,2',4'-pentahydroxyflavone) can selectively form a highly fluorescent complex with aluminum and has been used widely as a reagent for both fluorometric and spectrophotometric determinations. Morin dye has been used for Al (III) detection by reversed-phase high-performance liquid chromatography with fluorescence detection or in imprinted polymers either in immobilized or in free form (Lian H. Z. *et al.*, 2003, Al-Kindy S. *et al.*, 2002).

8-hydroxyquinolinesulfonic acid ligand has been used many times for optical Al(III) sensing by Brach-Papa&Coulomb (2002,2004).

Sing Muk Ng & R. Narayanaswamy, employed molecularly imprinted polymer (MIP) as a sensing receptor for Al^{3+} ion detection by using an optical approach. Al^{3+}ion was adopted as the template molecule and 8-hydroxyquinolinesulfonic acid ligand as the fluorescence tag. Gupta e*t al.* proposed an Al^{3+} selective potentiometric sensor based on morin in PVC matrix (Gupta *et al.,* 2007). This method worked over an activity range of 5.0 x 10^{-7} to 1.0 x 10^{-1} M of Al^{3+}.

In this study, fluorescent dye, N-N'-bis (2-hydroxybenzylidene)-ethane-1,2-diamine was optically characterized in water, ethanol (EtOH), tetrahydrofuran (THF), Water :Ethanol mixture (To:EtOH 80:20), dichlorometan (DCM). The dye was tested for the determination of metal ions in aqueous solutions by spectrofluorimetric method. The dye exhibited promising optical characteristics such as high Stoke's shift value (110 nm). The pH dependency and metal sensing studies were performed in buffered aqueous solutions. The cross-sensitivity of the dye to Cu^{2+}, Ca^{2+}, Hg^{+}, Pb^{2+}, Cr^{3+}, Mn^{2+}, Mg^{2+}, Sn^{2+}, Fe^{3+}, Cd^{2+}, Co^{2+} , Zn^{2+} and Ni^{2+} was investigated in separate solutions. The dye exhibited very selective increasing emission based response to Al(III) ions in the concentration range of 5.4-54.0 ppm in acetic acid/acetate buffer.

4.2 Experimental

4.2.1 Materials

Absolute ethanol, THF, DCM, and nitric acid (HNO_3) were of analytical grade. Solvents for the spectroscopic studies were used without further purification.
Buffer components were of analytical grade (Merck and Fluka). For metal ion tests, **AAS** Standard solutions of Mn^{2+}, Hg^{2+}, Hg^{+}, Fe^{2+}, Cr^{3+}, Mn^{2+}, Mg^{2+}, Sn^{2+}, Cd^{2+}, Co^{2+}, Ni^{+2}, Zn^{+2} and Ca^{2+} (1000 mg/ L, Merck) were diluted with 0.01 M sodium acetate buffer of pH 5.0 and ultra pure water. Solutions of Al (III) were prepared from the respective metal nitrate and diluted with 0.01 M sodium acetate buffer of pH 5.0. The pH values of the solutions were checked using a digital pH meter (WTW) calibrated with standard buffer solutions of Merck. All the experiments were

carried out at room temperature; 25 ˚C. The synthesis of Y1 dye has been performed in our laboratories by Associated Prof. Dr. M. Yavuz Ergun. Schematic structure of the employed dye molecule is shown in Fig. 4.1.

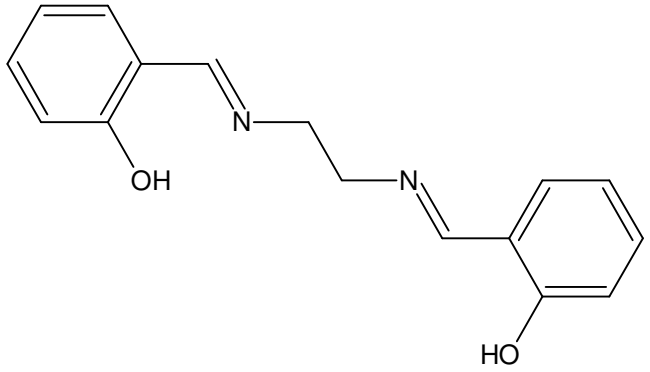

Figure 4.1 N-N'-bis (2-hydroxybenzylidene)-ethane-1,2-diamine (Y1)

4.2.2 Instrumentation

Absorption spectra were recorded using a Shimadzu 1601 UV-Visible spectrophotometer. Steady state fluorescence emission and excitation spectra were measured using Varian Cary Eclipse Fluorescence Spectrophotometer with a Xenon flash lamp as the light source. pH measurements were recorded with a WTW pH meter. In all of the studies, ultra pure water of Millipore was used.

4.3 Result and Discussion

4.3.1 Spectral Response of Y1

Spectral characterization data of Y1 in the solvents of EtOH, DCM, THF and in water ethanol mixture were obtained by means of absorption and emission spectrometry. Figure 4.2 and table 4.1 reveal absorption based spectral response of Y1 dye in the solvents of EtOH, DCM, THF, water and in water ethanol mixture.

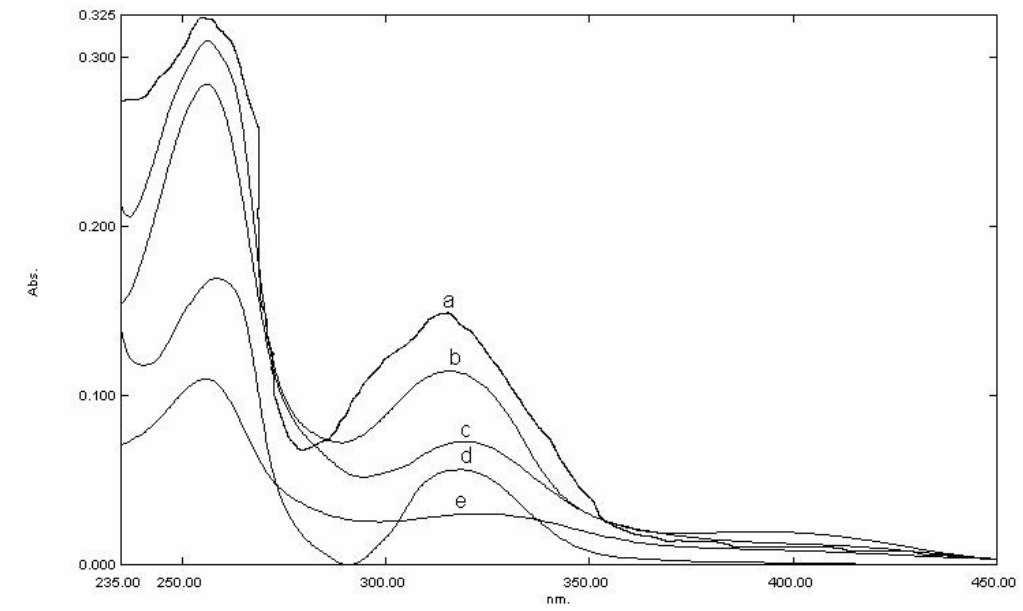

Figure 4.2 Absorbstion spectra of Y1 in the solvents of EtOH, DCM, THF, water and in water ethanol mixture. a) Y1 in THF b) Y1 in EtOH c) Y1 in water ethanol mixture d) Y1 in DCM e) Y1 in water

The indicator dye N-N'-bis (2-hydroxybenzylidene)-ethane-1,2-diamine (Y1) exhibited different molar extinction coefficients in the employed solvents (ε=11400M $^{-1}$ cm^{-1} in ethanol (λ_{max} : 316 nm), ε=7300 M $^{-1}$ cm^{-1} in water- ethanol mixture (λ_{max}: 320 nm), ε=5600 M $^{-1}$ cm^{-1} in DCM (λ_{max} : 317 nm), ε=3000 M $^{-1}$ cm^{-1} in water (λ_{max}: 322 nm), ε=17100 M $^{-1}$ cm^{-1} in THF (λ_{max}: 312 nm)). Among them the responses obtained in ethanol and THF were the best.

Table 4.1 Spectral characterization of Y1 dye (λ_{ex} : excitation wavelength in nm, λ_{em} : emission wavelength in nm, $\Delta\lambda_{ST}$: Stoke's shift and θ_F : Quantum yield)

Compound	Solvent	λ^{ex}_{max} *(excitation wavelength)*	λ^{em}_{max} (emission wavelength)	$\Delta\lambda_{ST}$ (Stoke's shift)	θ_F (Quantum yield)
Y1	DCM	292	322	30	0.072 in EtOH
	THF	265	328	63	
	EtOH	343	421	78	
	water	290	330	40	
	water : eth	380	490	110	

The Y1 dye exhibited different Stoke's shift values extending from 30 to 110 nm. Stoke's shift is important for fluorescence and optical sensor studies because the high Stoke's shift value allows the emitted fluorescence photons to be easily distinguished from the excitation photons, leading to the possibility of very low background signals and permits the usage of indicator dye in the construction of fiber optic sensor. The Stoke's shift value at least 30 nm is required for optical sensor design. The Stoke's shift value of 110 nm, acquired in water-ethanol mixture for Y1 is proper for optical sensing studies performed with fiber optic probes.

The indicator dye Y1 could not be doped into the PVC due to the leaching tendency of the dye. Therefore spectral response of the Y1 dye was evaluated in water or water-ethanol mixtures.

4.3.2 Quantum Yield Calculations of Y1

The fluorescence quantum yield of Y1 dye in EtOH was calculated by William's Method. The Williams method and the calculation of quantum yield values was explained in detail in Chapter 2. For this purpose, the emission spectra of five different concentrations of reference standard (Quinin Sulphate) were recorded by exciting at 318 nm. By similar way, the emission spectra of the five different concentrations of the Y1 dye were recorded (See Figure 4.3).

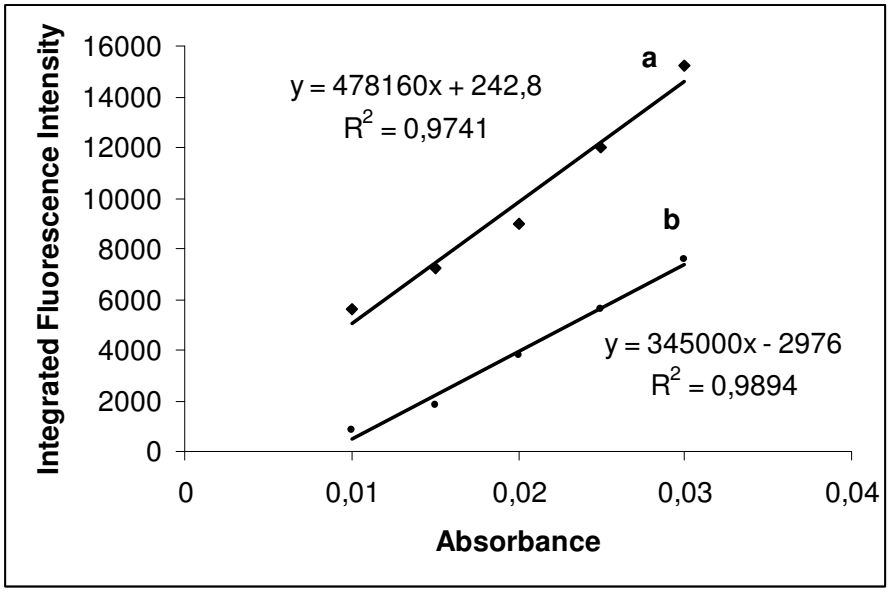

Figure 4.3 The integrated fluorescence intensities *vs* absorbance values of Y1 dye in EtOH (excitation at 318 nm). a: theintegrated fluoresence intensity of reference standard vs absorbance b: the integrated fluoresence intensity of unknown vs absorbance.

The integrated fluorescence intensities were plotted *vs.* absorbance for the reference standard, and the dye. The ratio of gradients of the plots is important and proportional to the quantum yield. The linearized plots of the reference standard and dye in EtOH can be described by equations and the relevant correlation coefficients of [y = 478160x + 242,8, R^2 = 0,9741] and [y = 345000x – 2976, R^2 = 0,9894], respectively. Fluorescence quantum yield of Y1 dye in EtOH was found to be, Q_f = 0.072. The calculated quantum yield value can be concluded as moderate.

4.3.3 pH Dependency of The Indicator Dye

Figure 4.4 reveals emission based response of the Y1 dye to pH in water-ethanol mixture. From Fig. 4.4 it can be concluded that the Y1 dye exhibits a very strong pH dependency between pH 8.0-12.0.

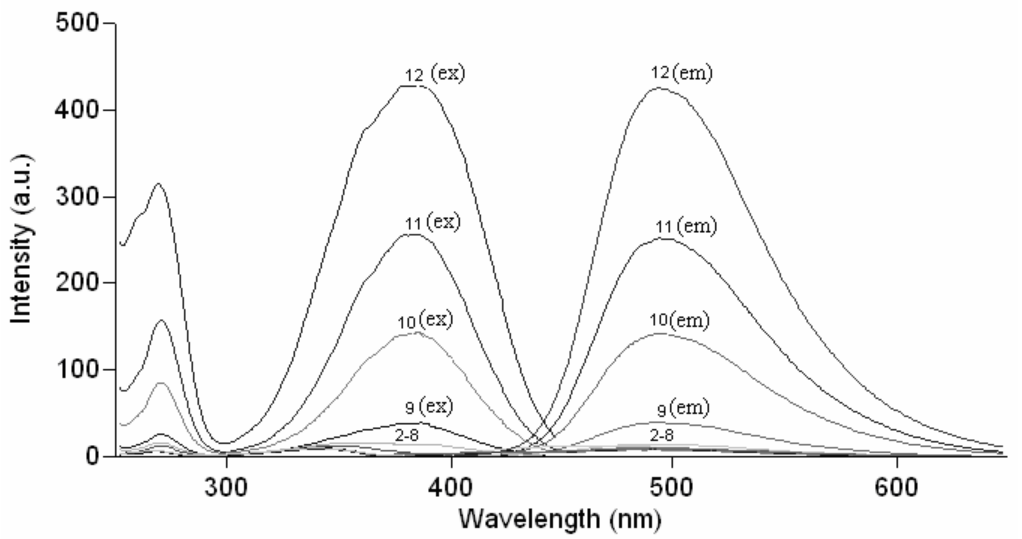

Figure 4.4 Excitation and emission based response of the Y1 dye to pH in water-ethanol mixture(90:10) in the pH range of 2.0-12.0.

Further studies were performed at pH 5.5 ; in acetic acid/acetate buffered solutions. This pH value was chosen due to the resistance of the dye to variations in pH. Table 4.2 reveals pH dependent forms of aluminum at pH 5.5.

Table 4.2 pH dependent distribution of aluminum at pH 5.5. (calculated with Visual MINTEQ)

Species Name	% of Total Component Concentration
Al^{3+}	39.805
$AlOH^{2+}$	39.558
$Al(OH)_2^+$	19.807
$Al(OH)_3$	0.792
$Al(OH)_4^-$	0.039

4.3.4 Response of Y1 Dye to Al^{3+}

Response of the Y1 dye to Al^{3+} has been tested and evaluated in water at pH 5.5. The Y1 dye exhibited a linear emission based response to Al^{3+} in the concentration range of $1x10^{-7}$-$1x10^{-2}$ M. Figure 4.4 - 4.6 reveal emission based increasing response of Y1 dye to Al^{3+} in the above mentioned concentration range.

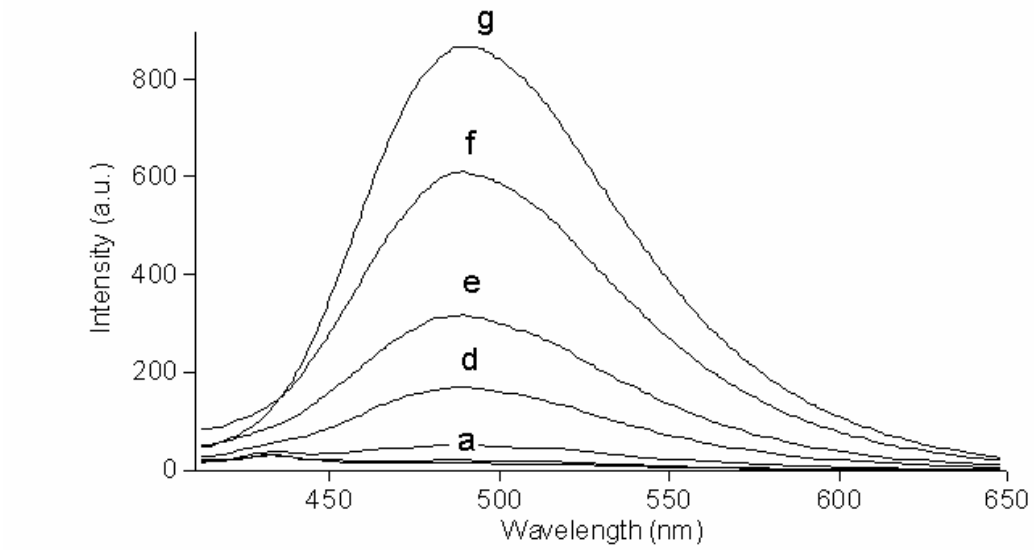

Figure 4.5 Emission based response of Y1 dye to Al^{3+} in the concentration range of $1x10^{-7}$-$1x10^{-2}$ M. (a: initial, b: 10^{-7}M Al^{3+} c- 10^{-6}M Al^{3+} d 10^{-5}M Al^{3+} e 10^{-4}M Al^{3+} f- 10^{-3}M Al^{3+} g- 10^{-2}M Al^{3+})

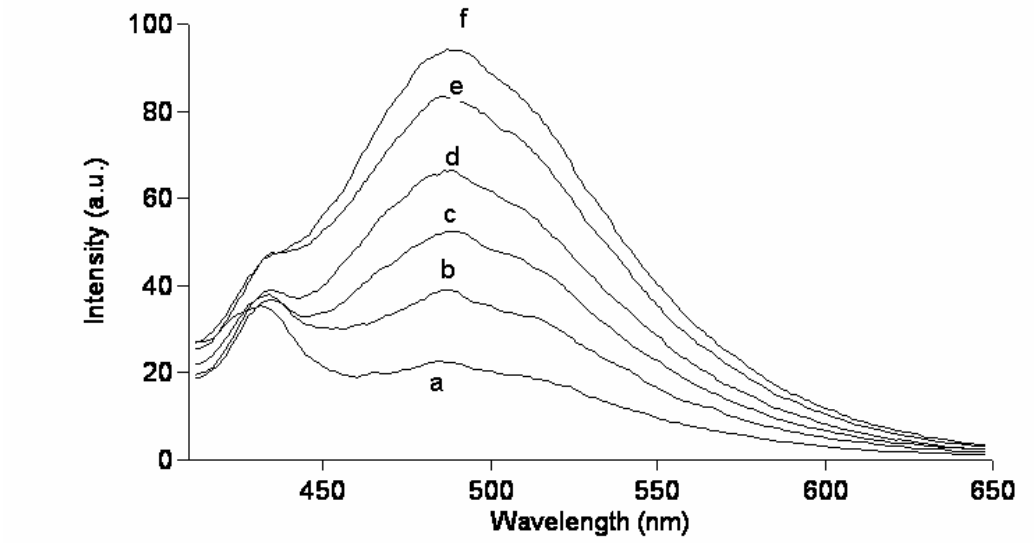

Figure 4.6 Emission based response of Y1 dye to Al^{3+} in the concentration range of $1x10^{-7}$-$1x10^{-6}$ M. (a: $1x10^{-7}$ b: $2x10^{-7}$ c: $4x10^{-7}$ d: $6x10^{-7}$ e: $8x10^{-7}$ f: $1x10^{-6}$ M)

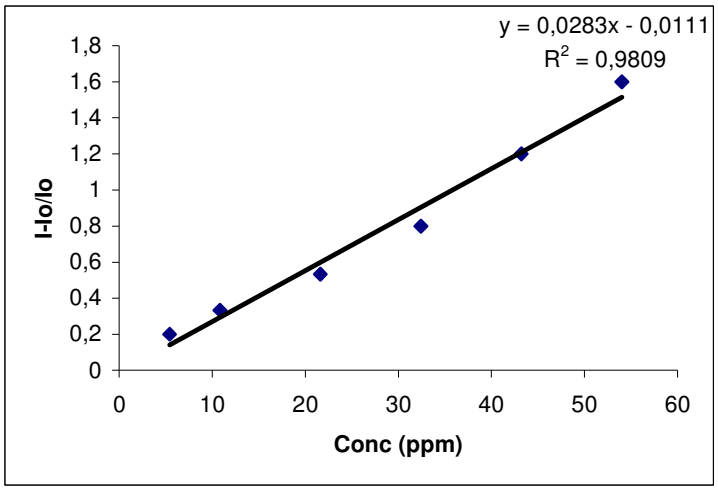

Figure 4.7: Linearized emission based response of Y1 dye to Al^{3+} in the concentration range of $1x10^{-7}$-1x10-^{6} M (5.4 - 54 ppm).

The linear response range of the Y1 dye can be concluded as $1x10^{-7}$-1x10-^{6} M.

4.3.5 Selectivity Studies

In order to examine the response of the Y1 dye to possible interfering cations, the sensor dye was treated with 10^{-3}M concentrations of Mn^{2+}, Hg^{2+}, Al^{3+}, Cr^{3+}, Mg^{2+}, Sn^{2+}, Cd^{2+}, Co^{2+}, Cu^{2+}, Ni^{2+}, Zn^{2+}, Bi^{2+} and Ca^{2+} ions in 0.01 M BES buffer solutions. From Fig. 4.8, it can be concluded that, the sensing dye solution is also capable of determining bismuth and copper ions (Bi^{2+} and Cu^{2+}) with a high selectivity over Mn^{2+}, Hg^{2+}, Al^{3+}, Cr^{3+}, Mg^{2+}, Sn^{2+}, Cd^{2+}, Co^{2+}, Cu^{2+}, Ni^{2+}, Zn^{2+}, Bi^{2+} and Ca^{2+}. However, the response to Al^{3+} is markedly different from the response to other metal ions and fluorescence of Y1 is affected appreciably by Al^{3+}.

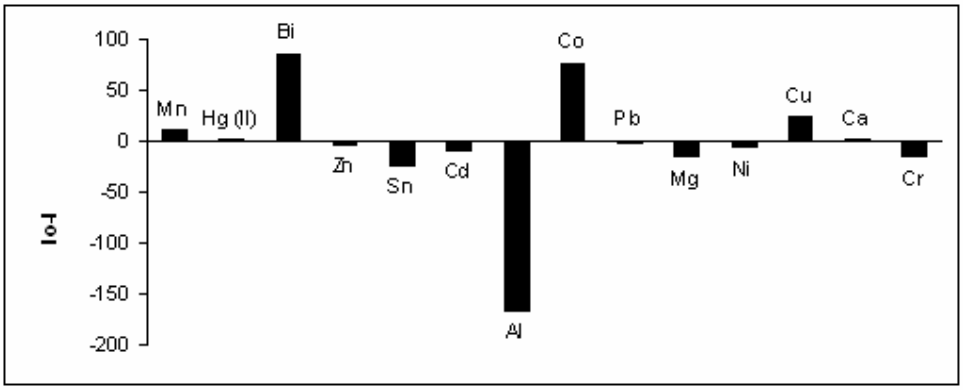

Figure 4.8 The response of the Y1 to possible interfering cations.

4.3.6 Absorption and Emission Based Response of Y1 to Al^{3+} in Ionic Liquid

Figure 4.9 and 4.10 reveal absorption and emission based response of Y1 to Al^{3+} in the water-miscible ionic liquid of 1- ethyl 3- methyl imidazolium tetrafluoroborate. There is a considerable response of Y1 to Al^{3+} in the ionic liquid. However, response is not reproducible. The system should be tuned but this will be the subject of another study.

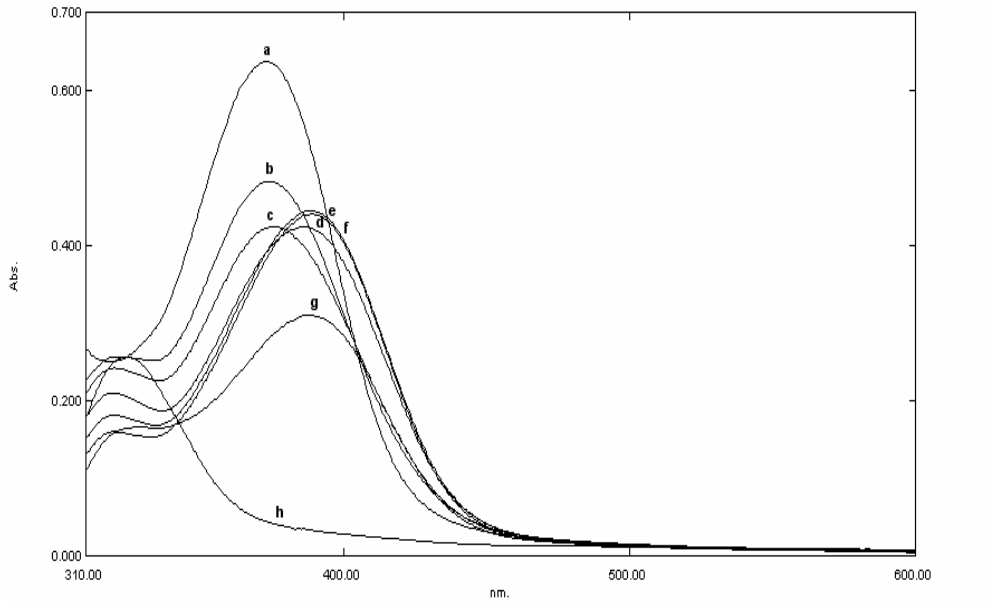

Figure 4.9 Absorption based response of Y1 to Al3+ in ionic liquid (a: initial; response in IL b- 10^{-9}M Al^{3+} c- 10^{-8}M Al^{3+} d- 10^{-7}M Al^{3+} e- 10^{-6}M Al^{3+} f- 10^{-5}M Al^{3+} g- 10^{-4}M Al^{3+} h- 10^{-3}M Al^{3+}).

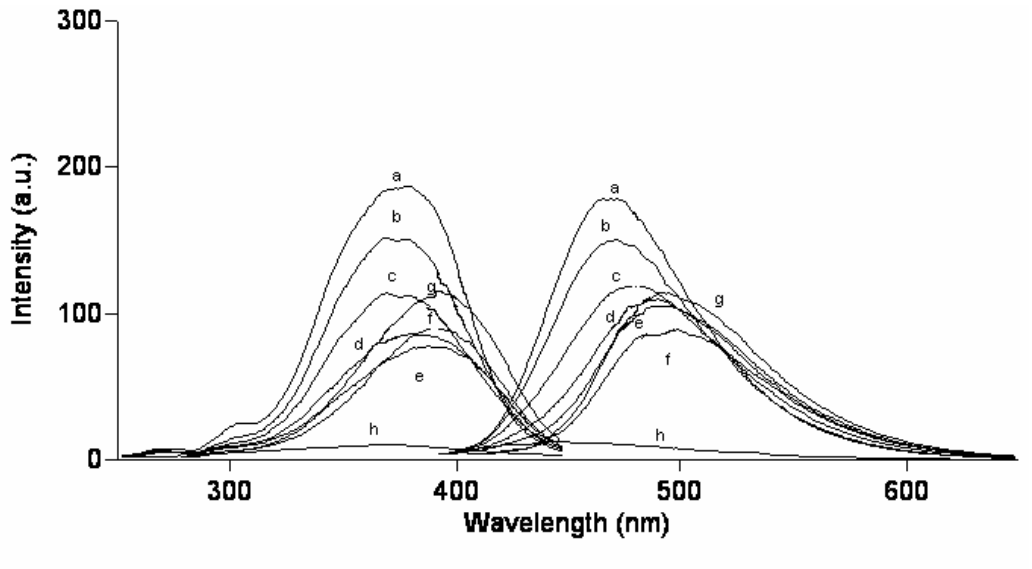

Figure 4.10 Emission based response of Y1 to Al3+ in ionic liquid (a: initial; response in IL b- 10^{-9}M Al^{3+} c- 10^{-8}M Al^{3+} d- 10^{-7}M Al^{3+} e- 10^{-6}M Al^{3+} f- 10^{-5}M Al^{3+} g- 10^{-4}M Al^{3+} h- 10^{-3}M Al^{3+}).

4.3.7 Complex Stochiometry of Al^{3+} with Y1

Information on the stoichiometry of the complex was obtained from the continuous variation method (Job's method). The method was employed as explained earlier.

Figure 4.11; Job's plot for the employed dye and metal; reveals complex formation between Y1 and Al^{3+} in ethanol. From the Job's plot for Al^{3+} stoichiometry of the metal–ligand complex was estimated as 2:3 at the employed total concentration; 1×10^{-5} mol l^{-1}.

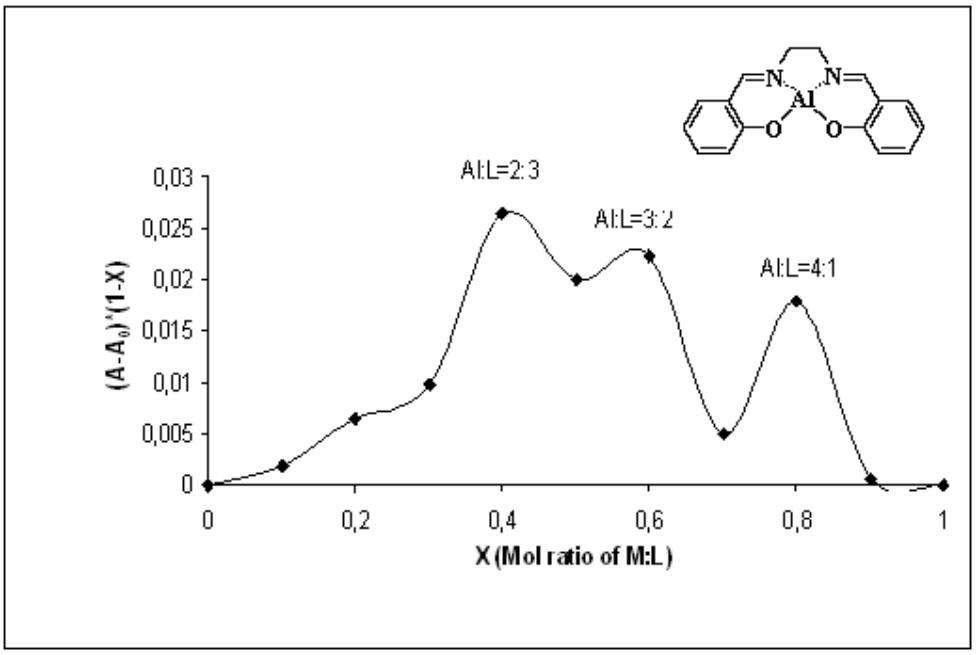

Figure 4.11; Job's plot for the employed dye; Y1 and metal.

4.4 Conclusion

In the second part of the thesis, an original Al^{3+} probe was tried to be developed. Organic fluoroionophore; N-N'-bis (2-hydroxybenzylidene)-ethane-1,2-diamine (Y1), was studied in various solvents (dichlorometan, tetrahydrofurane, toluen and ethanol) by using absorption and emission spectroscopy. Spectral response of dye to dissolved aluminium and pH and was investigated in to dept. The complex stoichiometry between dye and heavy metal was defined with Job's Method. The indicator dye Y1 exhibited relative signal change extending to 87 % in solution phase. The work described here demonstrates a selective fluorescence based molecular probe for Al^{3+} ions. To our knowledge the Y1 dye was used for the first time as a fluoroionophore in the optical aluminum sensing studies. The quantum yield of the dye in EtOH is reasonably high (0.072) and could be excited at visible region with commercially available cheap LEDs. The sensor can be used at pH 4.0 for quantitative determination of Al^{3+} in the concentration range of $1x10^{-7}$-1x10-^{2} M It's cross sensitivity to possible interferents were investigated by means of emission spectroscopy. From the above mentioned experimental results it can be concluded that, the sensing dye solution is also capable of determining bismuth and copper ions

(Bi^{+2} and Cu^{2+}) with a high selectivity over Mn^{2+}, Hg^{2+}, Al^{3+}, Cr^{3+}, Mg^{2+}, Sn^{2+}, Cd^{2+}, Co^{2+}, Cu^{2+}, Ni^{2+}, Zn^{2+}, Bi^{2+} and Ca^{2+}. However, the response to Al^{3+} is markedly different from the response to other metal ions and fluorescence of Y1 is affected appreciably by Al^{3+}.

REFERENCES

Akkaya E. U., & Turkyilmaz S. (1997). A squaraine-based near IR fluorescent chemosensor for Calcium. *Tetrahedron Letters*, 38 (25), 4513-4516

Aksuner, N. (2008). Development of New Optıcal Sensors for Metal Ion Sensing. Ege University Graduate School of Natural and Applied Sciences: Izmir

Al-Kindy, S., Badía, R., & Díaz-García, M. E. (2002). Fluorimetric monitoring of molecular imprinted polymer recognition events for aluminum. *Analytical Letters*, 35 (11), 1763 - 1774

Baker, S. N., Baker, G. A., & Bright, F. V. (2002) Temperature-dependent microscopic solvent properties of dry and wet 1-butyl-3-methylimidazolium hexafluorophosphate: correlation with ET(30) and Kamlet-Taft polarity scales. *Green Chemistry,* 4, 165–169.

Brach-Papa, C., Coulomb, B., Boudenne, J-L., Cerda, V. & Theraulaz, F. (2002). Spectrofluorimetric determination of aluminum in drinking waters by sequential injection analysis**.** *Analytica Chimica Acta,* 457, 311–318

Brach-Papa, C., Coulomb, B., Théraulaz, F., Van Loot, P., Boudenne, J-L, Branger, C. & Margaillan, A. (2004). Fluorimetric determination of aluminium in water by sequential injection through column extraction. *Analytical Bioanalytical Chemistry,* 378, 1652–1658.

Brennecke, J. F. & Maginn, E. J. (2001), Ionic liquids: innovative fluids for chemical processing. *AICHE Journals*, 47, 2384–2389.

Carmichael, A. J. & Seddon, K. R. (2000). Polarity study of some 1-alkyl-3-methylimidazolium ambient-temperature ionic liquids with the solvatochromic dye Nile red. *Journal of Physical Organic Chemistry,* 13, 591–595.

Constantini, S. & Giordano R. (M. Nicolini, P. F. Zatta & B. Corain, Eds) (1991). In "Aluminum in Chemistry, Biology and Medicine". Cortina Int. : Verona

Coskun, A., Deniz, E., & Akkaya E. U. (2007). A sensitive fluorescent chemosensor for anions based on a styryl–boradiazaindacene framework. *Tetrahedron Letters*, 48 (31), 5359-5361

Deng, Z., Coudray, C., Gouzoux, L., Mazur, A., Rayssiguier, Y. & Pepin, D. (1998). Effect of oral aluminum and aluminum citrate on blood level and short-term tissue distribution of aluminum in the rat. *Biological Trace Element Research,* 63, 139-147.

Derinkuyu, S., Ertekin, K., Oter, O., Denizalti, S., & Cetinkaya, E. (2007). Fiber optic pH sensing with long wavelength excitable Schiff bases in the pH range of 7.0–12.0. *Analytica Chimica Acta,* 588, 42–49

Dhami, S., Mello A. J., Rumbles, G., Bishop, S. M., Phillips, D. & Beeby, A. (1995). Phthalocyanine fluorescence at high concentration: dimers or reabsorption effect? *Photochemistry and Photobiology,* 61, 341.

Eisenrich, S. J. (1980). Atmospheric input of trace metals to Lake Michigan. *Water Air Soil Pollution,* 13,287-302.

Ensafi, A. A. & Aboutalebi, A. (2005). A versatile stable cobalt optical sensor based on pyrogallol red immobilization on cellulose acetate film. *Sensors & Actuators, Chemicals B*, 105 (2), 479-485.

Ensafi, A. A. & Bakhshi, M. (2003). New Stable Optical Film Sensor Based on Immobilization of 2-Amino-1-Cyclopentene-1-Dithiocarboxylic Acid on Acetyl Cellulose Membrane for Ni(II) Determination. *Sensors and Actuators B: Chemicals*, 96 (1-2), 435-440.

Flaten, T. P. (2001). Aluminum as a risk factor in Alzheimer's disease, with emphasis on drinking water. *Brain Research Bulletin,* 55, 187-196.

Filipek, L. H., Nordstorm, D. K. & Ficklin, W. H. (1987). Interaction of acid mine drainage with waters and sediments of West Squaw Creek in the West Shasta mining district, California. *Environmental Science & Technology,* 21, 388-396.

Gankema, H., Lugtenberg, R.J.W., Engbersen, J.F.J., Reinhoudt, D. N & Moller, M. (1994). Cross-linkable polar siloxane copolymers for ion detection devices. *Advanced Materials*, 6 (12): 944-947.

Gündüz, T. (2002). Instrumental Analiz. Gazi Kitabevi : Ankara, 278-280

Gupta V. K., Jain A. K., & Maheshwari G. (2007). Aluminum(III) selective potentiometric sensor based on morin in poly(vinyl chloride) matrix. *Talanta* 72 (4), 1469-1473

Harris, W. R., Berthon, G., Day, J. P., Exley, C., Flaten, T. P., Forbes, W. F., Kiss, T., Orvig, C. & Zatta, P. F. (1996). Speciation of aluminum in biological system. *Journal of Toxicology and Environmental Health,* 48, 543-568.

Huang, C. C. & Chang, H. T. (2006). Selective gold-nanoparticle-based "turn-on" fluorescent sensors for detection of mercury(II) in aqueous solution. *Analytical Chemistry,* 78 (24)**,** 8332-8338.

Hulanicki, A., Geab, S. & Ingman, F. (1991). Chemical Sensors Definitions and Classification. *Pure & Application Chemistry,* 63(9), 1247-1250.

Ittel, T. H. (1993). Determinants of gastrointestinal absorption and distribution of aluminum in health and uraemia. *Nephrol Dial Transplant,* 8, 17-24.

Koch, K. R., Pougnet, M. A. B., Villiers, S. D. & Montegudo, F. (1988). Increased urinary excretion of aluminum after drinking tea. *Nature,* 333,122.

Lee, R. E., von Lehmden, D. J. (1973). Trace metal pollution in the environment. *Journal of the Air Pollution Control Association*, 23, 853- 857.

Levesque, L., Mizzen, C. A., McLahlan, D. R. & Fraser, P. E. (2000). Ligand species effects on aluminum incorporation and toxicity in neurons and astrocytes. *Brain Research,* 887, 191-202.

Lian H., Kang Y., Bi S., Yasin A., Shao D., Chen Y., Dai L., & Tian L. (2003).Morin applied in speciation of aluminium in natural waters and biological samples by reversed-phase high-performance liquid chromatography with fluorescence detection. *Analytical Bioanalytical Chemistry*, 376, 542–548.

Matsumoto, H. (2000). Cell biology of aluminum toxicity and tolerance in higher plants. *International Review of Cytology,* 200, 1-46

Mercury (n.d.). Retrieved July 1,2008, from http://www.lenntech.com/periodic-chart-elements/hg-en.htm/

Mohr, G. J. (23th August, 2006).*A general introduction into optical sensor materials and recognition mechanism.online.* 18th July, 2008, http://www2.uni-jena.de/~c1moge/Mohr/ASCOS2002.pdf).

Murkovic, I., Lobnik, A., Mohr, G. J. & Wolfbeis, O. S. (1996). Fluorescent potential-sensitive dyes for use in solid state sensors for potassium ion. *Analytica Chimica Acta,* 334(1-2), 125-132.

Oter, O. (2007). Investigation of Sensor Characteristics of Some Chromoionophore Structures in Polymer and Sol-Gel Matrices. Dokuz Eylul University Graduate School of Natural and Applied Sciences: Izmir

Park, S. & Kazlauskas, R. (2003). Biocatalysis in ionic liquids—advantages beyond green technology. *Current Opinion in Biotechnol*ogy, 14, 432–437.

Rantwijk, F., Lau, R. M., & Sheldon, R. A. (2003). Biocatalytic transformations in ionic liquids. *Trends Biotechnology,* 21, 131–138.

Seddon, K. R, Stark, A., & Torres M. J. (2000). Influence of chloride, water, and organic solvents on the physical properties of ionic liquids. *Pure&Application Chemistry*, 72, 2275–2287.

Sing Muk, Ng *&* Narayanaswamy, R. (2006). Fluorescence sensor using a molecularly imprinted polymer as a recognition receptor for the detection of aluminium ions in aqueous media. *Analytical Bioanalytical Chemistry*, 386,1235–1244.

Sorrenson, J. R. J., Campbell, I. R., Teper, L. B. & Lingg, R. D. (1974). Aluminum in the environment and human health. *Environmental Health Perspectives*, 8, 3-95

U. S. Public Health Service (1992). Toxicological Profile for Aluminum and Compounds. Prepared by Clement International Corp. Contact No: 205-88-0608

Williams, A. T. R., Winfield, S. A. & Miller, J. N. (1983). Relative fluorescence quantum yields using a computer controlled luminescence spectrometer. *Analyst*, 108, 1067.

Wolfbeis, O. S. (Ed.) (1991). Fiber Optic Chemical Sensors and Biosensors. *CRC* Press: London.

Wolfbeis, O. S. & Weidgans, B. M. (2006). Fiber Optic Chemical Sensors and Biosensors: A View Back. *Springer Netherlands*, 224, 17-44.

World Food and Nutrition Study (1977). *National Academy of Sciences*, 11, 74-84.

Yang, Z. & Pan, W. (2005). Ionic liquids: Green solvents for nonaqueos biocatalysis. *Enzyme and Microbial Technology*, 37, 19–28.